Supercomputer Simulations of Galaxy Formation

Volker Springel

MAX PLANCK INSTITUTE
FOR ASTROPHYSICS

Physics Colloquium
CERN
March 24, 2024

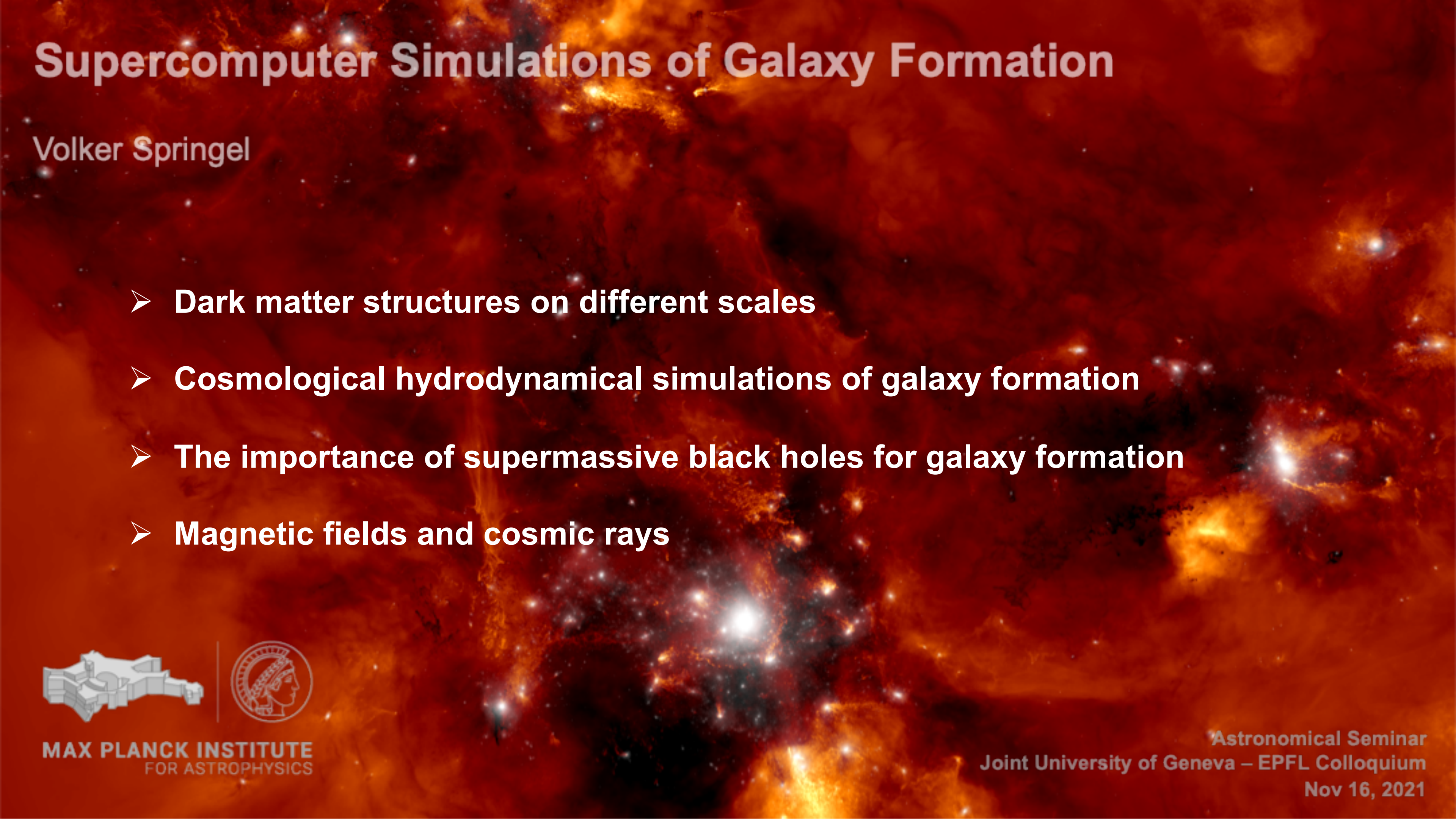

Supercomputer Simulations of Galaxy Formation

Volker Springel

- ➢ Dark matter structures on different scales
- ➢ Cosmological hydrodynamical simulations of galaxy formation
- ➢ The importance of supermassive black holes for galaxy formation
- ➢ Magnetic fields and cosmic rays

MAX PLANCK INSTITUTE
FOR ASTROPHYSICS

Astronomical Seminar
Joint University of Geneva – EPFL Colloquium
Nov 16, 2021

Amazing observational progress has specified the intial conditions

COSMIC MICROWAVE BACKGROUND CONTRAINTS AS SEEN BY PLANCK

Minimal, 6-parameter ΛCDM model is a great fit

Planck Collaboration (2018)

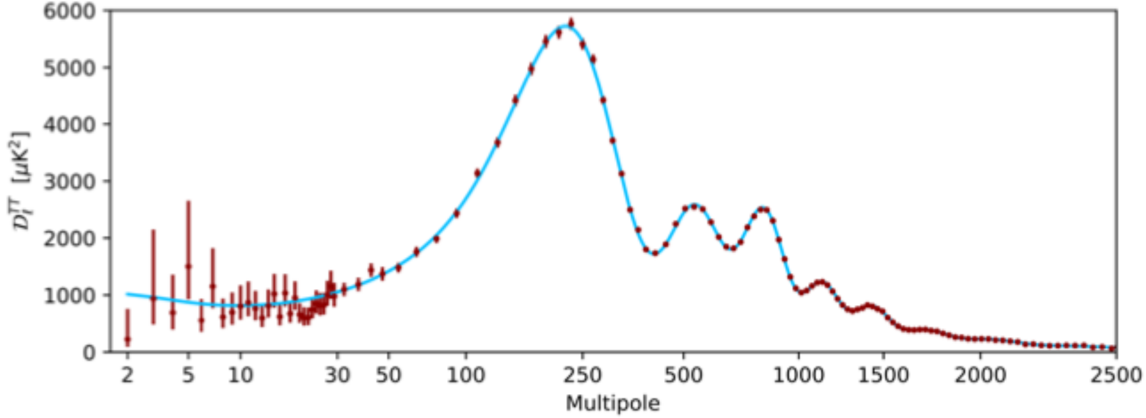

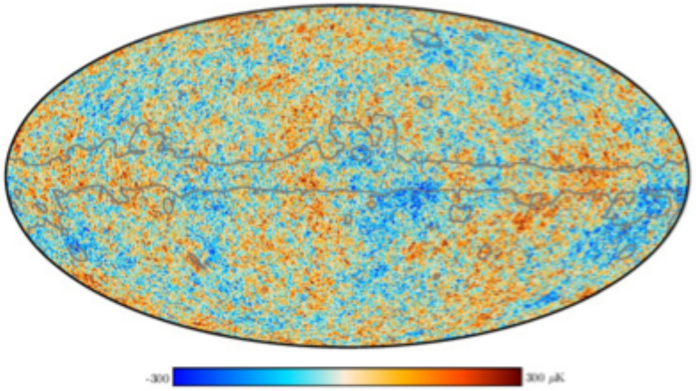

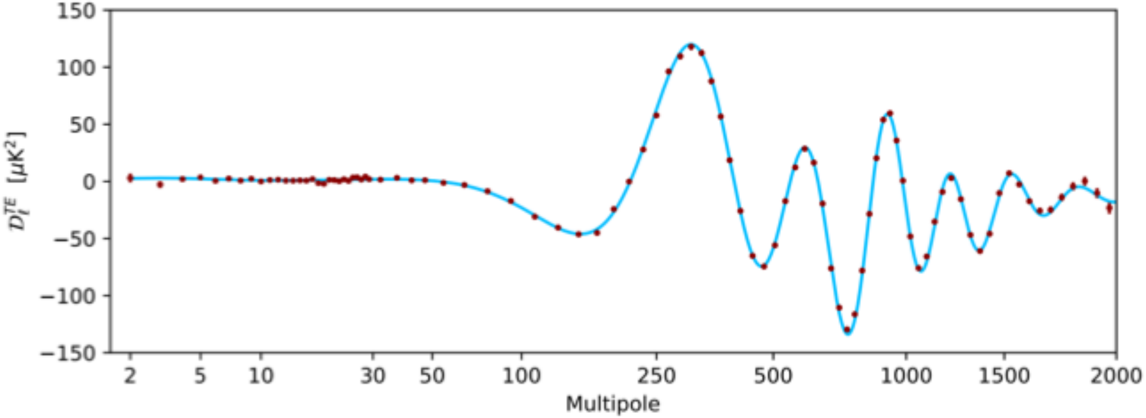

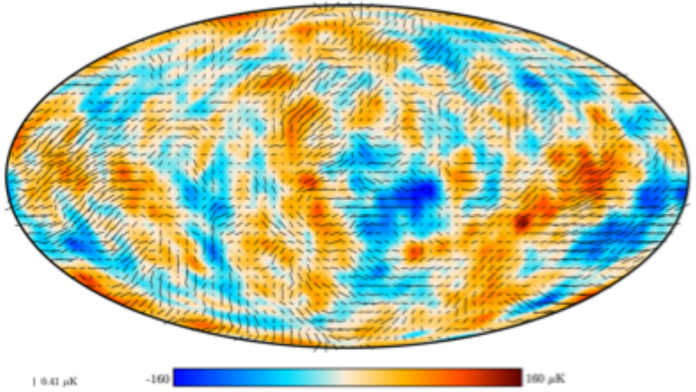


Hoag's Object


M104


NGC 1300

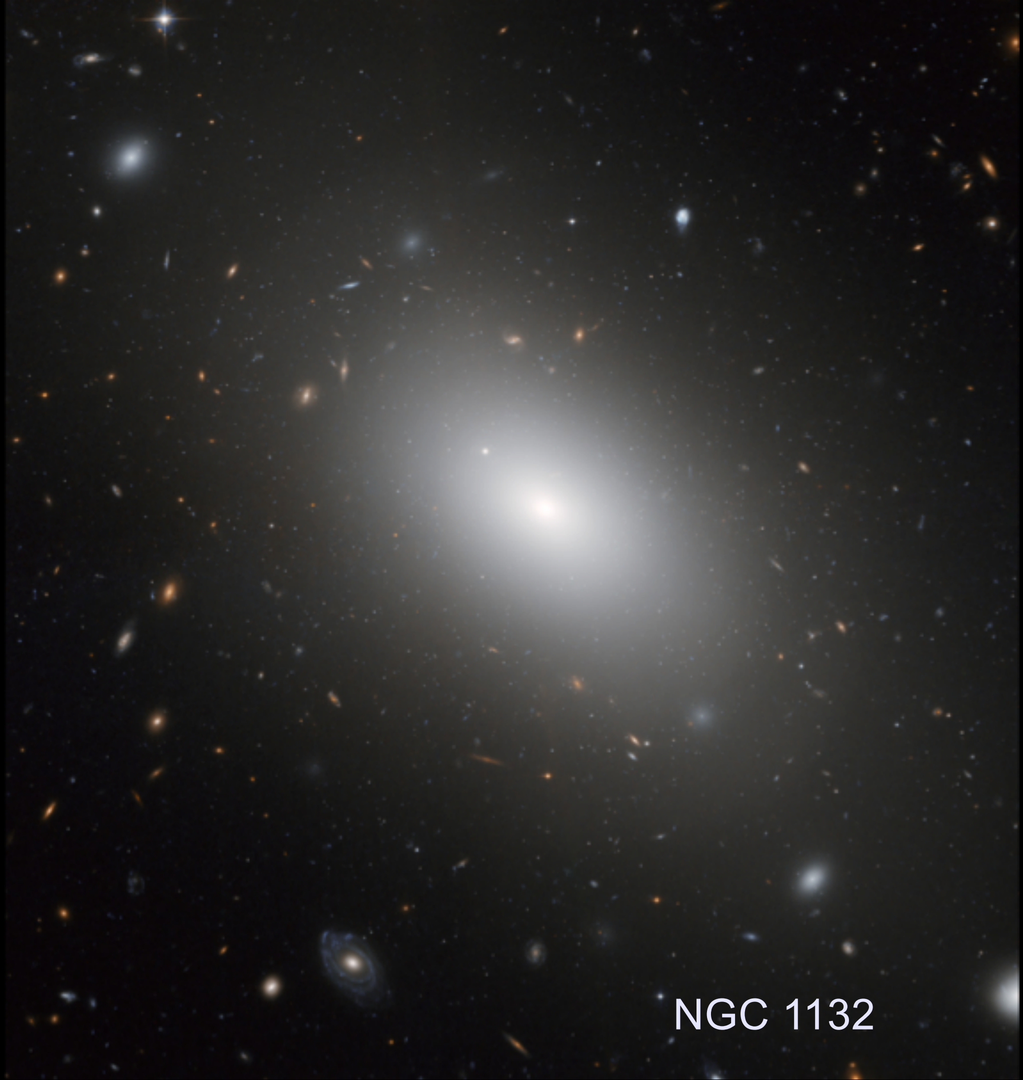
NGC 1132

Observed galaxy distribution in the Universe

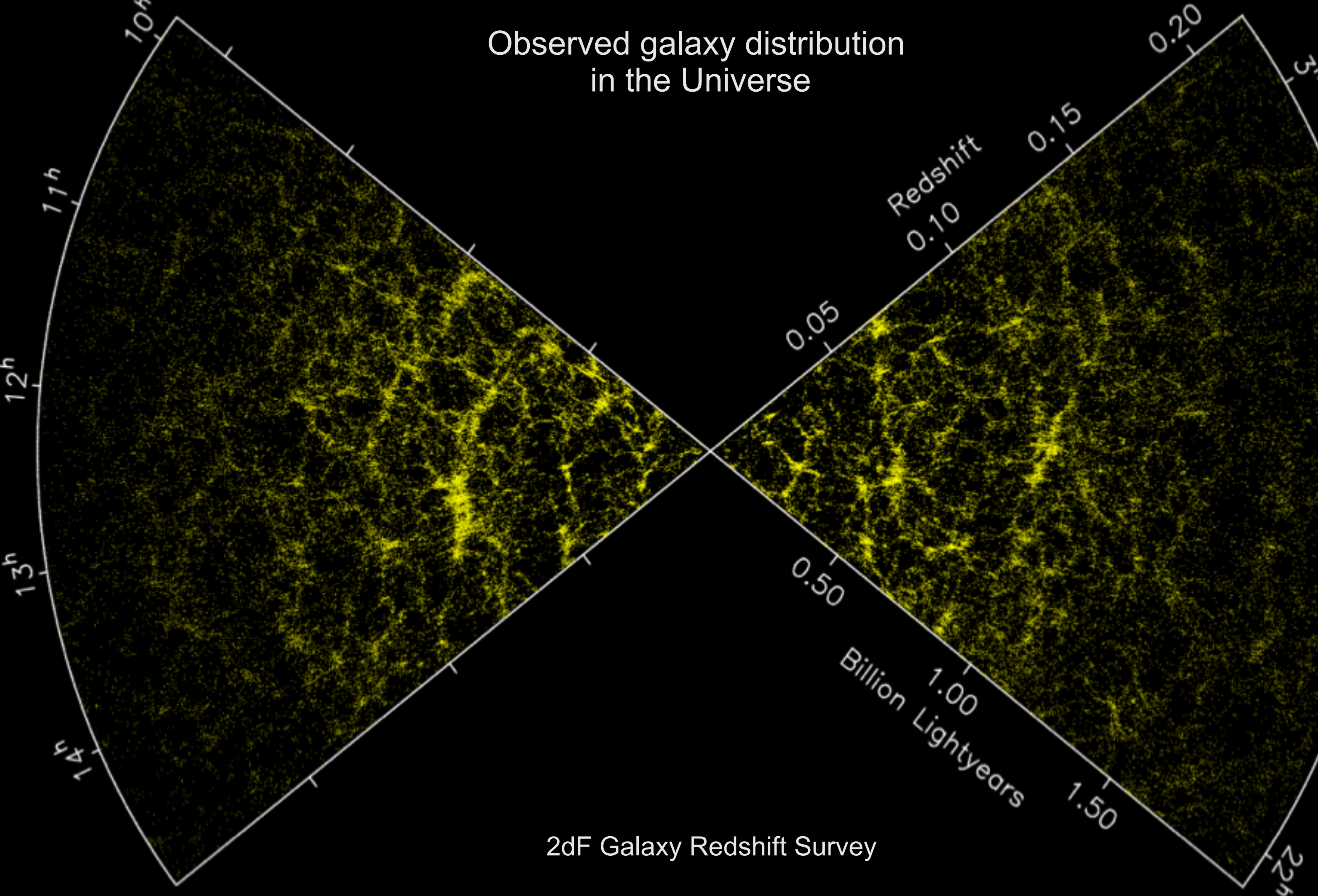

2dF Galaxy Redshift Survey

Hubble Ultra Deep Field

Need to bridge 13.7 billion years of (non-linear) evolution

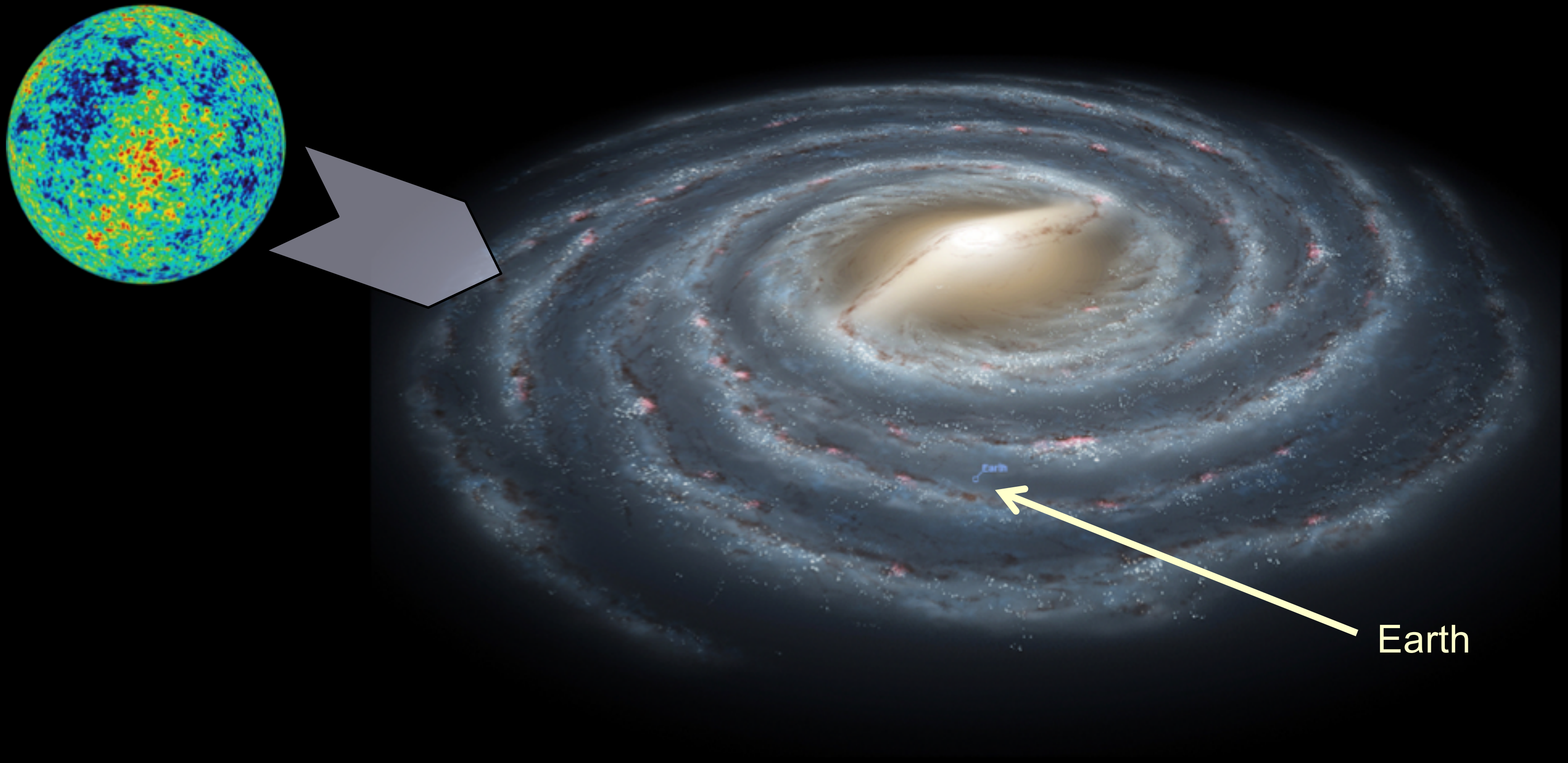

Much of astrophysics is fully described by systems of Partial Differential Equations

THE PHYSICS ONLY FULLY REVEALED THROUGH SOLUTIONS OF THESE EQUATIONS IN NON-TRIVIAL SITUATIONS

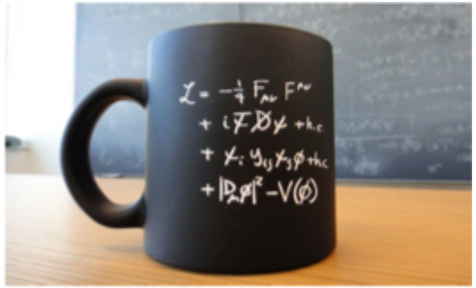

hyperbolic conservation laws of fluid dynamics

$$\frac{\partial \rho}{\partial t} + \nabla(\rho \mathbf{v}) = 0$$

$$\frac{\partial}{\partial t}(\rho \mathbf{v}) + \nabla(\rho \mathbf{v}\mathbf{v}^T + P) = \nabla \mathbf{\Pi}$$

$$\frac{\partial}{\partial t}(\rho e) + \nabla[(\rho e + P)\mathbf{v}] = \nabla(\mathbf{\Pi}\mathbf{v})$$

- Euler/Navier-Stokes equations for the gas
- Vlasov equation for collisionless dark matter
- Radiative transfer
- Magnetohydrodynamics
- General relativity
- ….

Poisson-Vlasov system

$$\frac{\mathrm{d}f}{\mathrm{d}t} = \frac{\partial f}{\partial t} + \frac{\partial f}{\partial \mathbf{x}} \cdot \mathbf{v} + \frac{\partial f}{\partial \mathbf{v}} \cdot \left(-\frac{\partial \Phi}{\partial \mathbf{x}} \right) = 0$$

$$\nabla^2 \Phi(\mathbf{x}, t) = 4\pi G \int f(\mathbf{x}, \mathbf{v}, t)\, \mathrm{d}\mathbf{v}$$

rendered on SuperMUC by LRZ

Pretending that all cosmic matter is collisionless gives simplified models for structure growth

TREATING ORDINARY MATTER AS DARK MATTER

Composition of the Universe today (Planck ΛCDM model)

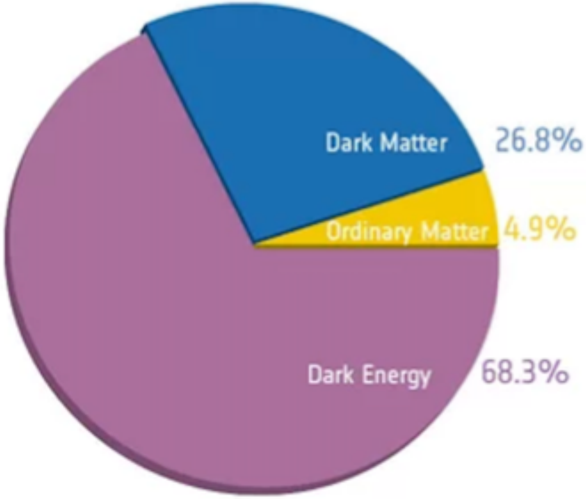

Fiducial Dark Matter-Only Universe

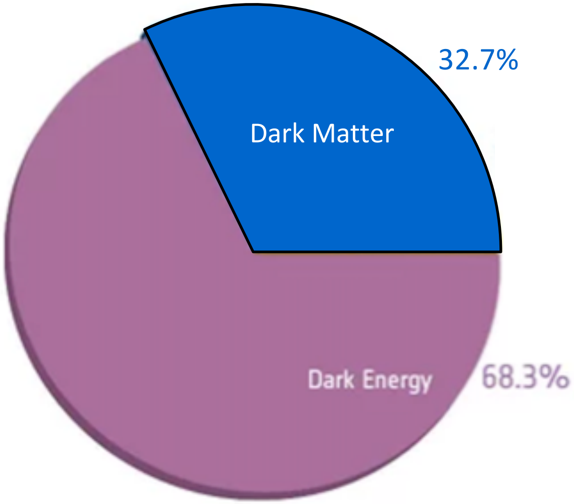

Springel et al. (2008)

Cosmological N-body simulations have been instrumental for understanding the non-linear outcome of ΛCDM

COSMIC LARGE-SCALE STRUCTURE IN DARK MATTER

Springel et al. (2005)

The structure of the smallest halos at z=0 has been resolved

PUSHING THE DYNAMIC RANGE OF COSMOLOGICAL N-BODY SIMULATIONS TO THE EXTREME WITH THE VVV SIMULATIONS

- Planck cosmology
- Dark matter only
- All simulations have 500 Mpc/h box
- Final zoom has dynamic range of 30 orders of magnitude in mass
- Best zoom reaches mass resolution of 10^{-11} solar masses

Wang, Bose, et al. (2020)

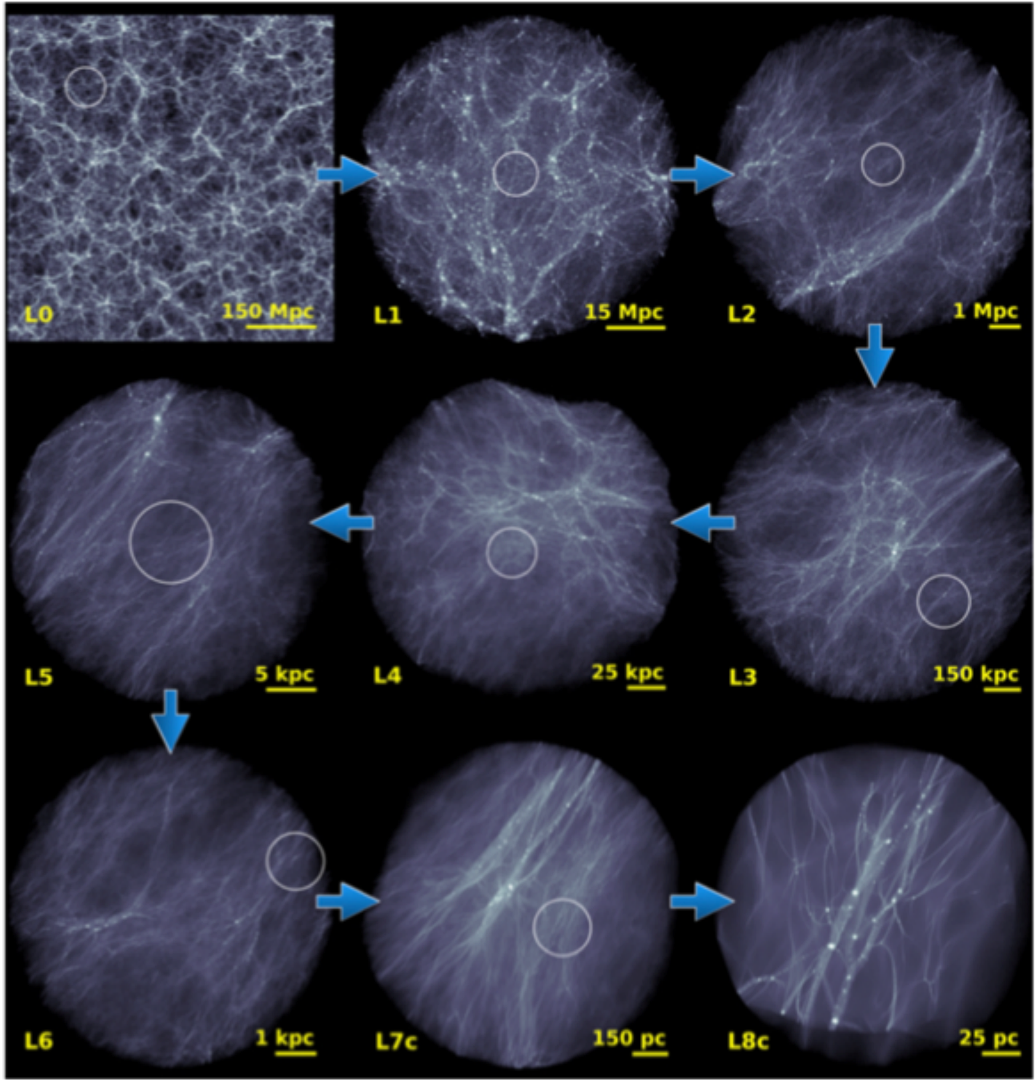

The mass-concentration relation shows a much weaker trend with halo mass than predicted by most theoretical models

CONCENTRATION VS HALO MASS

- Measured for the first time over the full 20 orders of magnitude populated for a 100 GeV WIMP

- There is a turndown at 1000 Earth masses due to the free-streaming limit.

- The scatter does not depend strongly on halo mass.

- Well-described by the Ludlow et al. (2016) model

Wang, Bose, et al. (2020)

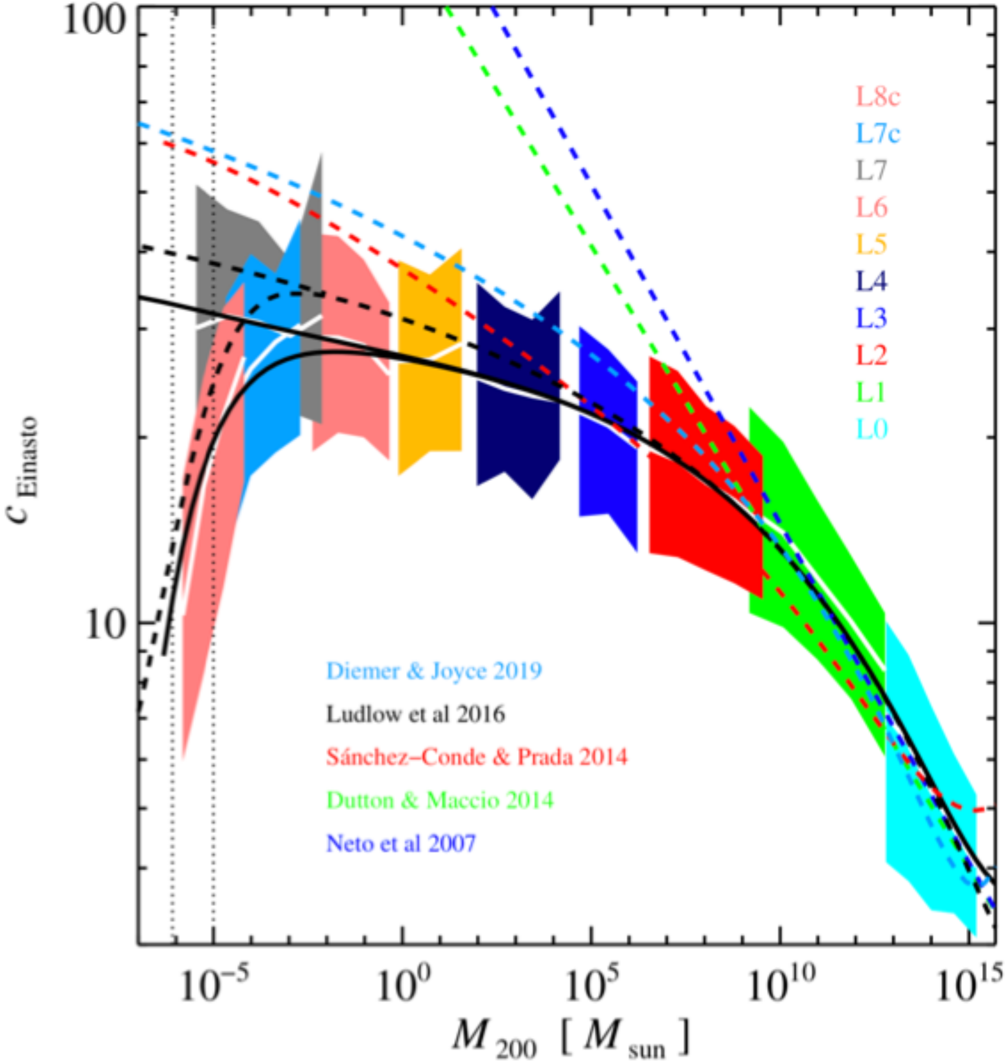

Hydro simulations…

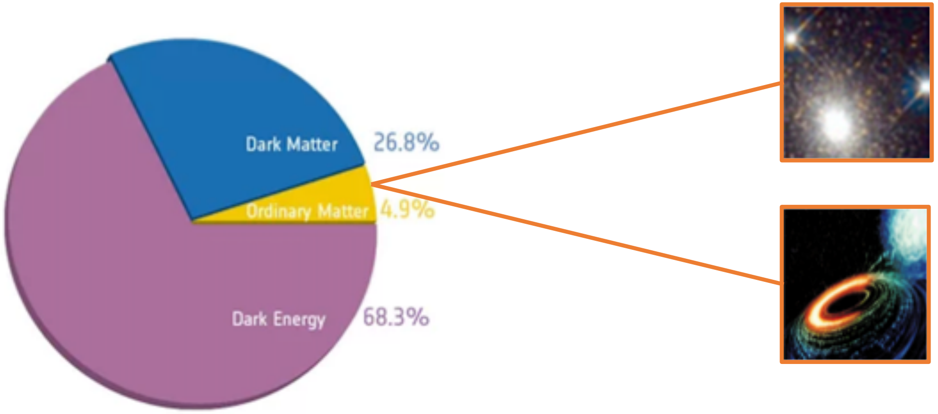

Stars 0.5%

Black holes 0.001%

aim to address the full problem

The **moving-mesh hydrodynamics AREPO** is well matched to cosmic structure formation

APPROACH AND PRINCIPAL ADVANTAGES

Springel (2010)

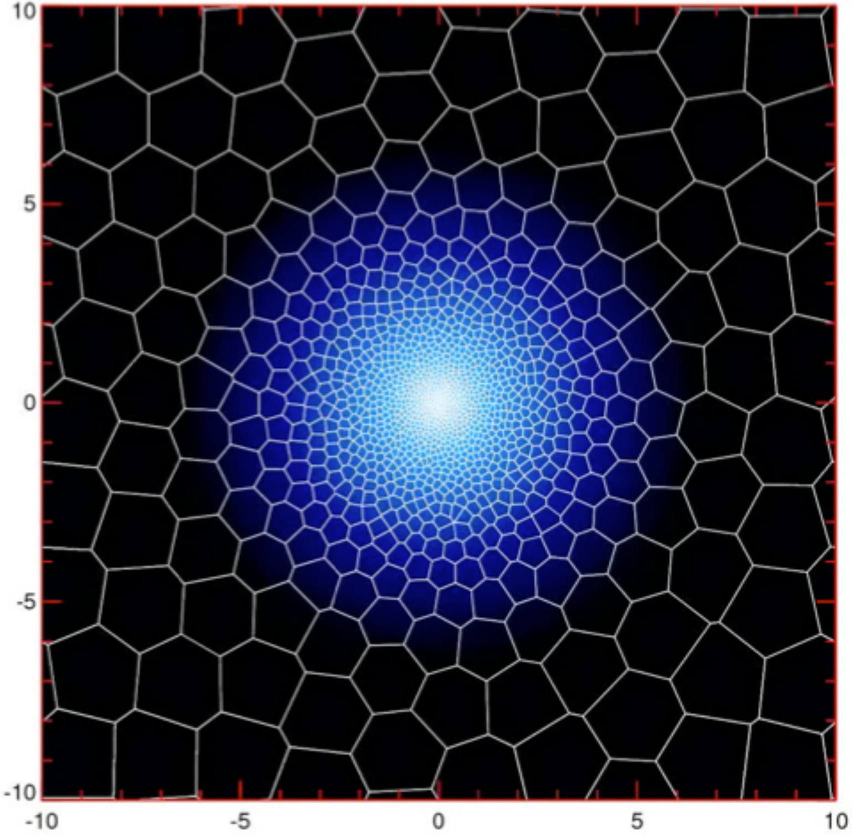

- Low numerical viscosity, very low advection errors
- Full adaptivity and manifest Galilean invariance
- Makes larger timesteps possible in supersonic flows

Sketch of flux calculation

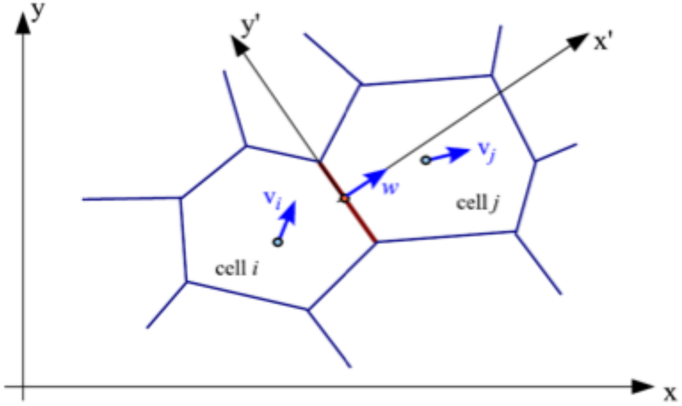

The motion of the mesh generators uniquely determines the motion of all cell boundaries

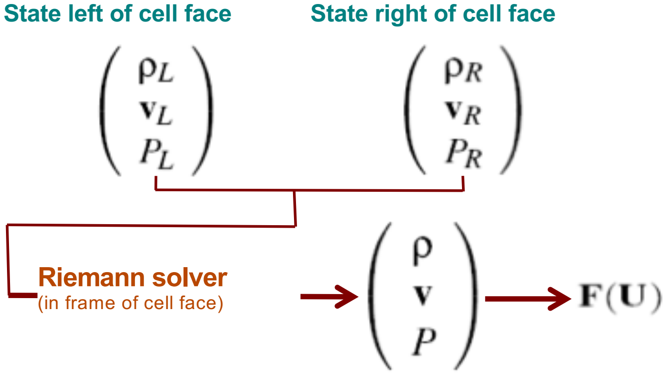

State left of cell face

$$\begin{pmatrix} \rho_L \\ \mathbf{v}_L \\ P_L \end{pmatrix}$$

State right of cell face

$$\begin{pmatrix} \rho_R \\ \mathbf{v}_R \\ P_R \end{pmatrix}$$

Riemann solver
(in frame of cell face)

$$\rightarrow \begin{pmatrix} \rho \\ \mathbf{v} \\ P \end{pmatrix} \rightarrow \mathbf{F}(\mathbf{U})$$

Galaxy Formation Physics in the Illustris / IllustrisTNG Simulations

THE MOST IMPORTANT MODELLING ASPECTS

Cooling and metal enrichment

- Nine elements followed independently
- Mass and metal loss of stars treated continuously over time based on stellar population synthesis models (similar to Wirsma et al. 2009)
- Ionization balance and cooling from H and He followed with direct chemical network (Katz et al. 1996)
- Metal line cooling added through CLOUDY tables in density, temperature and redshift
- Simple self-shielding correction (Rahmati et al. 2013)

Star formation and winds

- Variant of Springel & Hernquist (2003)
- Cold dense gas stabilized by an ISM equation of state
- Winds are phenomenologically introduced, with an energy given as a fixed fraction of the supernova energy
- The wind velocity is variable, the mass flux follows for energy-driven winds
- Fiducial model scales wind with local dark matter velocity dispersion
- Winds are launched outside of star-forming gas, and metal-loading can be reduced if desired

Black hole accretion and feedback

- Black hole seeding and accretion model (Springel et al. 2005)
- Quasar-mode feedback for high accretion rates
- Radio-mode feedback for low accretion rates based on bubble-heating model (Sijacki et al. 2006)
- Radiative AGN feedback (change in heating/cooling due to variation of UVB) in proximity to an active black hole
- Reduction of accretion rate in low-pressure/low-density regimes to avoid large hot bubbles around black holes in quiescent state
- Black holes tied to potential minimum of halos

New or modified in IllustrisTNG

- Magnetic fields
- New model for AGN radio mode (kinetic BH feedback)
- Slightly modified parameterization of supernova feedback
- Improved metal enrichment model

Zoom into the Illustris-Simulation…

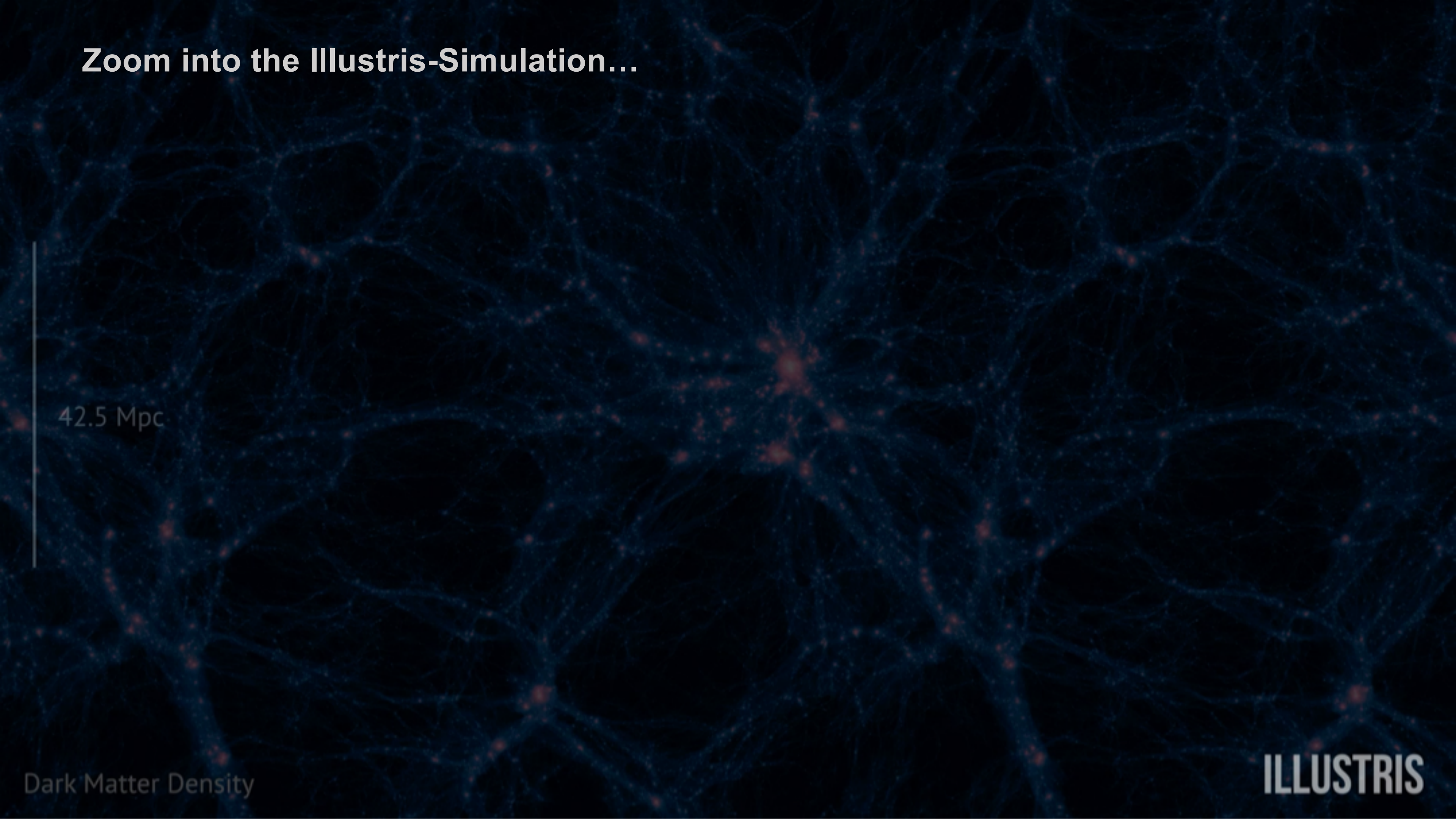

The “Next Generation Illustris Simulations” (IllustrisTNG) are our novel, significantly improved models for cosmic structure formation

DIFFERENT SIMULATIONS OF THE ILLUSTRIS-TNG PROJECT

IllustrisTNG Collaboration (2018)

data for TNG50/100/300 fully publicly available

426 papers thus far

(and 236 for Illustris)

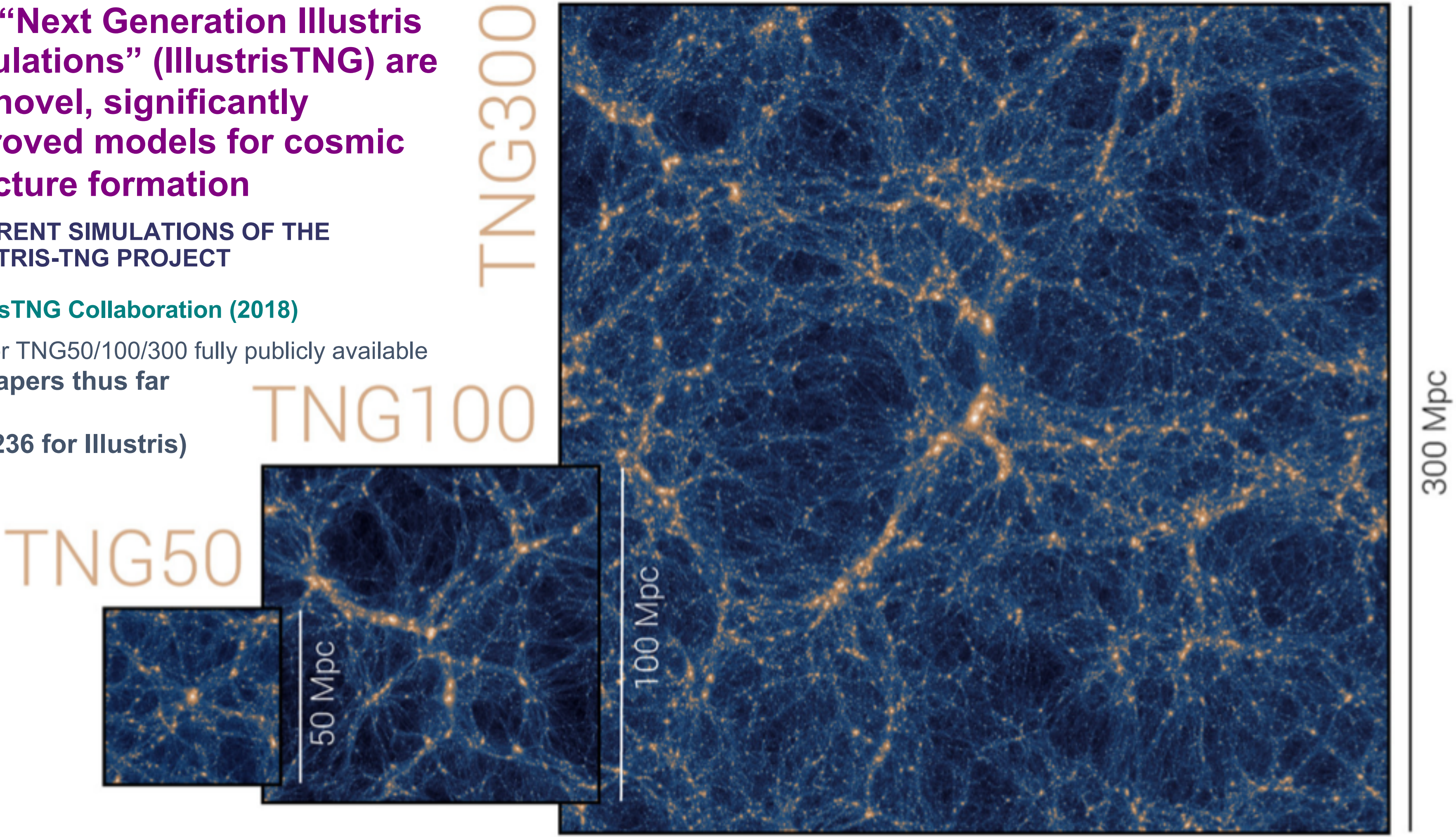

People in IllustrisTNG – “The Next Generation Illustris Simulations”

A COLLABORATION BETWEEN GARCHING, HEIDELBERG, HARVARD, AND THE MIT

Volker Springel

Heidelberg Institute for Theoretical Studies
PI: Overall TNG Project

Lars Hernquist

Harvard University

Annalisa Pillepich

Max Planck Institute for Astronomy, Heidelberg
Co-PI: TNG50 Project

Rüdiger Pakmor

Heidelberg Institute for Theoretical Studies

Dylan Nelson

Max Planck Institute for Astrophysics, Garching
Co-PI: TNG50 Project

Rainer Weinberger

Heidelberg Institute for Theoretical Studies

Federico Marinacci

Massachusetts Institute of Technology

Jill Naiman

Harvard University

Mark Vogelsberger

Massachusetts Institute of Technology

Shy Genel

Center for Computational Astrophysics, Flatiron Institute

Paul Torrey

Massachusetts Institute of Technology

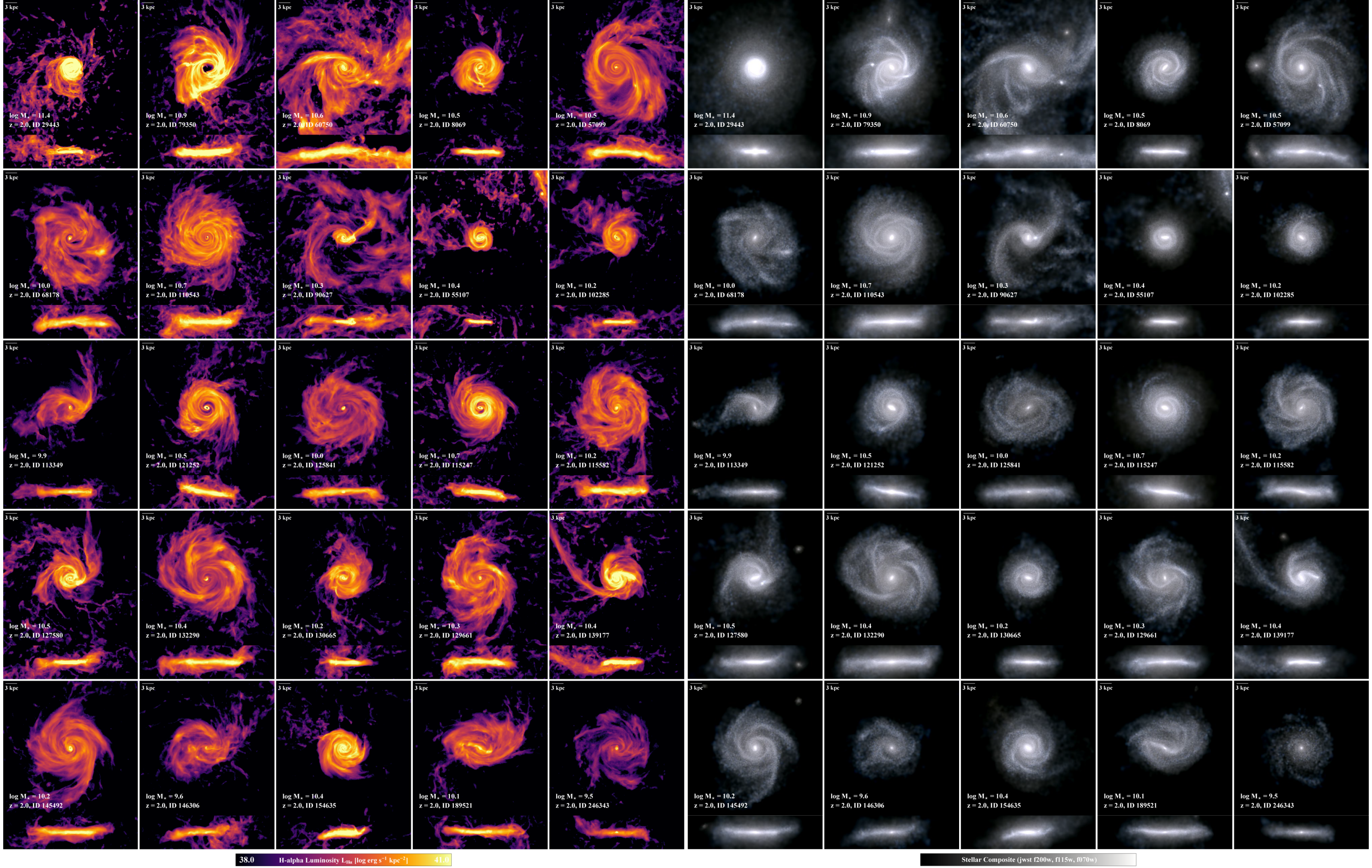
3 kpc
log M* = 11.4
z = 2.0, ID 29443
3 kpc
log M* = 10.9
z = 2.0, ID 79350
3 kpc
log M* = 10.6
z = 2.0, ID 60750
3 kpc
log M* = 10.5
z = 2.0, ID 8069
3 kpc
log M* = 10.5
z = 2.0, ID 57099
3 kpc
log M* = 11.4
z = 2.0, ID 29443
3 kpc
log M* = 10.9
z = 2.0, ID 79350
3 kpc
log M* = 10.6
z = 2.0, ID 60750
3 kpc
log M* = 10.5
z = 2.0, ID 8069
3 kpc
log M* = 10.5
z = 2.0, ID 57099
3 kpc
log M* = 10.0
z = 2.0, ID 68178
3 kpc
log M* = 10.7
z = 2.0, ID 110543
3 kpc
log M* = 10.3
z = 2.0, ID 90627
3 kpc
log M* = 10.4
z = 2.0, ID 55107
3 kpc
log M* = 10.2
z = 2.0, ID 102285
3 kpc
log M* = 10.0
z = 2.0, ID 68178
3 kpc
log M* = 10.7
z = 2.0, ID 110543
3 kpc
log M* = 10.3
z = 2.0, ID 90627
3 kpc
log M* = 10.4
z = 2.0, ID 55107
3 kpc
log M* = 10.2
z = 2.0, ID 102285
3 kpc
log M* = 9.9
z = 2.0, ID 113349
3 kpc
log M* = 10.5
z = 2.0, ID 121252
3 kpc
log M* = 10.0
z = 2.0, ID 125841
3 kpc
log M* = 10.7
z = 2.0, ID 115247
3 kpc
log M* = 10.2
z = 2.0, ID 115582
3 kpc
log M* = 9.9
z = 2.0, ID 113349
3 kpc
log M* = 10.5
z = 2.0, ID 121252
3 kpc
log M* = 10.0
z = 2.0, ID 125841
3 kpc
log M* = 10.7
z = 2.0, ID 115247
3 kpc
log M* = 10.2
z = 2.0, ID 115582
3 kpc
log M* = 10.5
z = 2.0, ID 127580
3 kpc
log M* = 10.4
z = 2.0, ID 132290
3 kpc
log M* = 10.2
z = 2.0, ID 130665
3 kpc
log M* = 10.3
z = 2.0, ID 129661
3 kpc
log M* = 10.4
z = 2.0, ID 139177
3 kpc
log M* = 10.5
z = 2.0, ID 127580
3 kpc
log M* = 10.4
z = 2.0, ID 132290
3 kpc
log M* = 10.2
z = 2.0, ID 130665
3 kpc
log M* = 10.3
z = 2.0, ID 129661
3 kpc
log M* = 10.4
z = 2.0, ID 139177
3 kpc
log M* = 10.2
z = 2.0, ID 145492
3 kpc
log M* = 9.6
z = 2.0, ID 146306
3 kpc
log M* = 10.4
z = 2.0, ID 154635
3 kpc
log M* = 10.1
z = 2.0, ID 189521
3 kpc
log M* = 9.5
z = 2.0, ID 246343
3 kpc
log M* = 10.2
z = 2.0, ID 145492
3 kpc
log M* = 9.6
z = 2.0, ID 146306
3 kpc
log M* = 10.4
z = 2.0, ID 154635
3 kpc
log M* = 10.1
z = 2.0, ID 189521
3 kpc
log M* = 9.5
z = 2.0, ID 246343
38.0
H-alpha Luminosity L_Hα [log erg s^-1 kpc^-2]
41.0
Stellar Composite (jwst f200w, f115w, f070w)

IllustrisTNG reproduces the color-bimodality of galaxies thanks to AGN feedback

COLOR DISTRIBUTION OF GALAXIES OF DIFFERENT MASS COMPARED TO SDSS

Nelson et al. (2017)

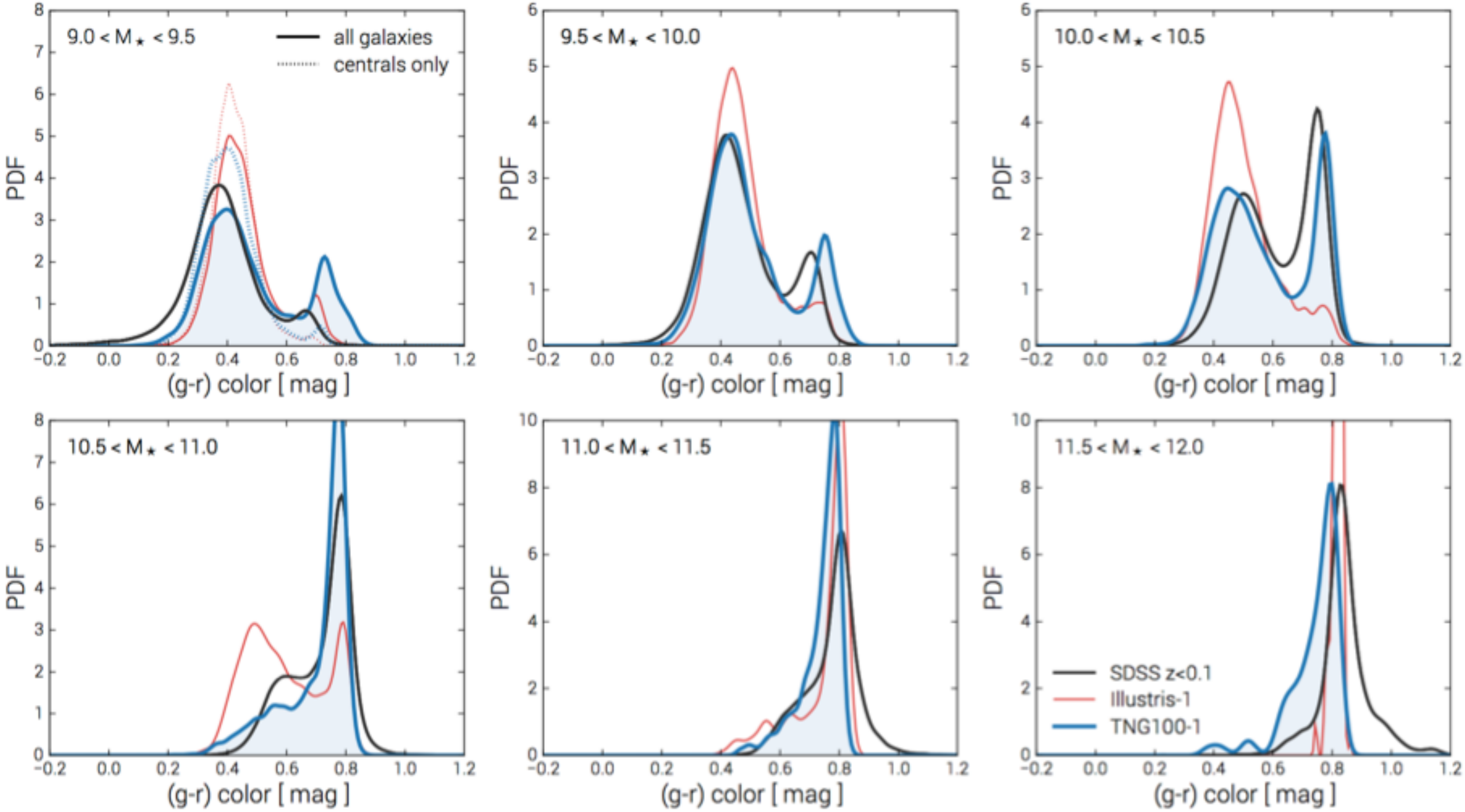

The sizes of different galaxies types reproduce observed trends with stellar mass well

ILLUSTRIS-TNG GALAXY SIZES AS A FUNCTION OF STELLAR MASS

Genel et al. (2018)

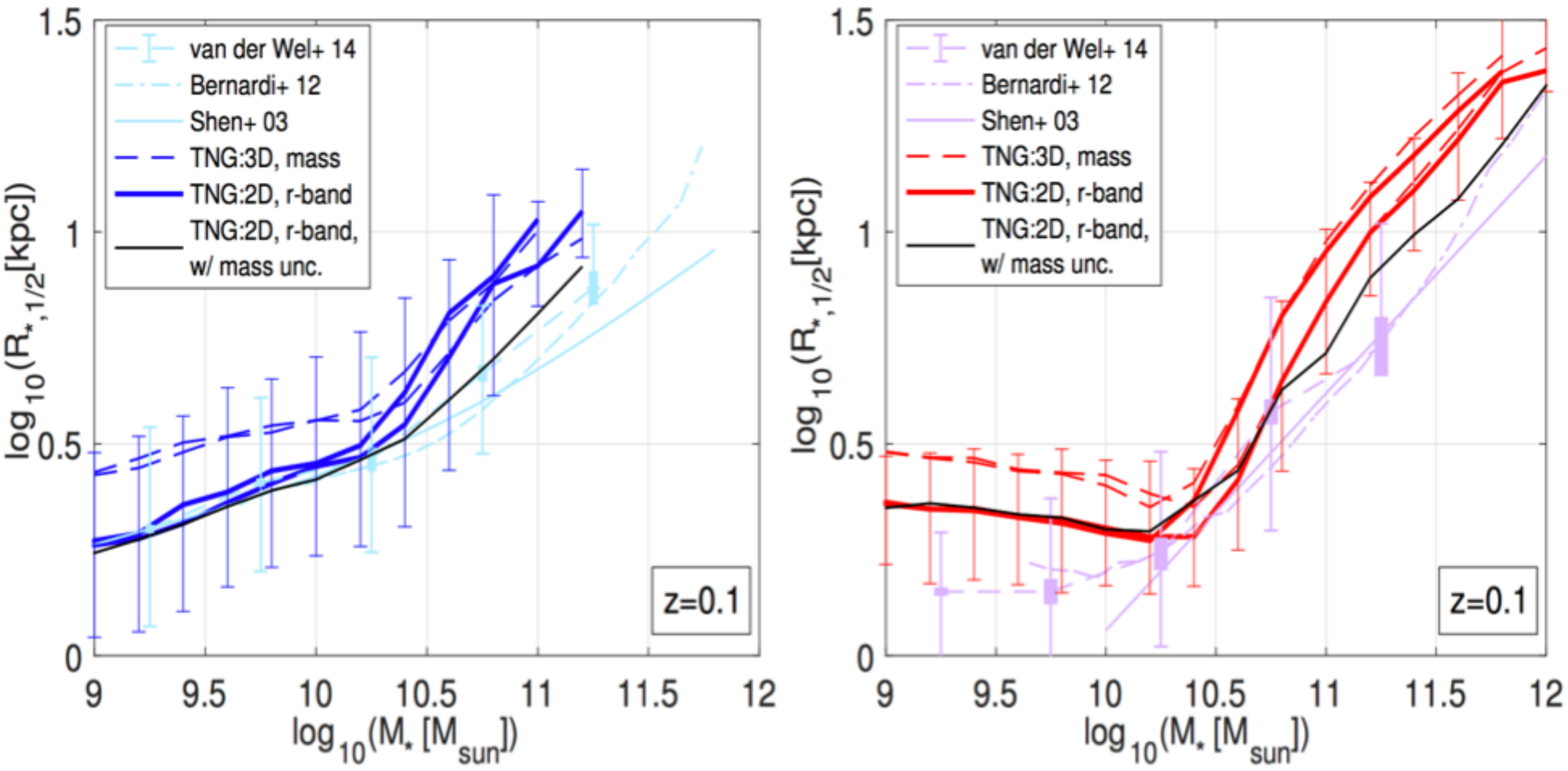

(a) Main-sequence / late-type galaxies

(b) Quenched / early-type galaxies

Large-scale structure in IllustrisTNG

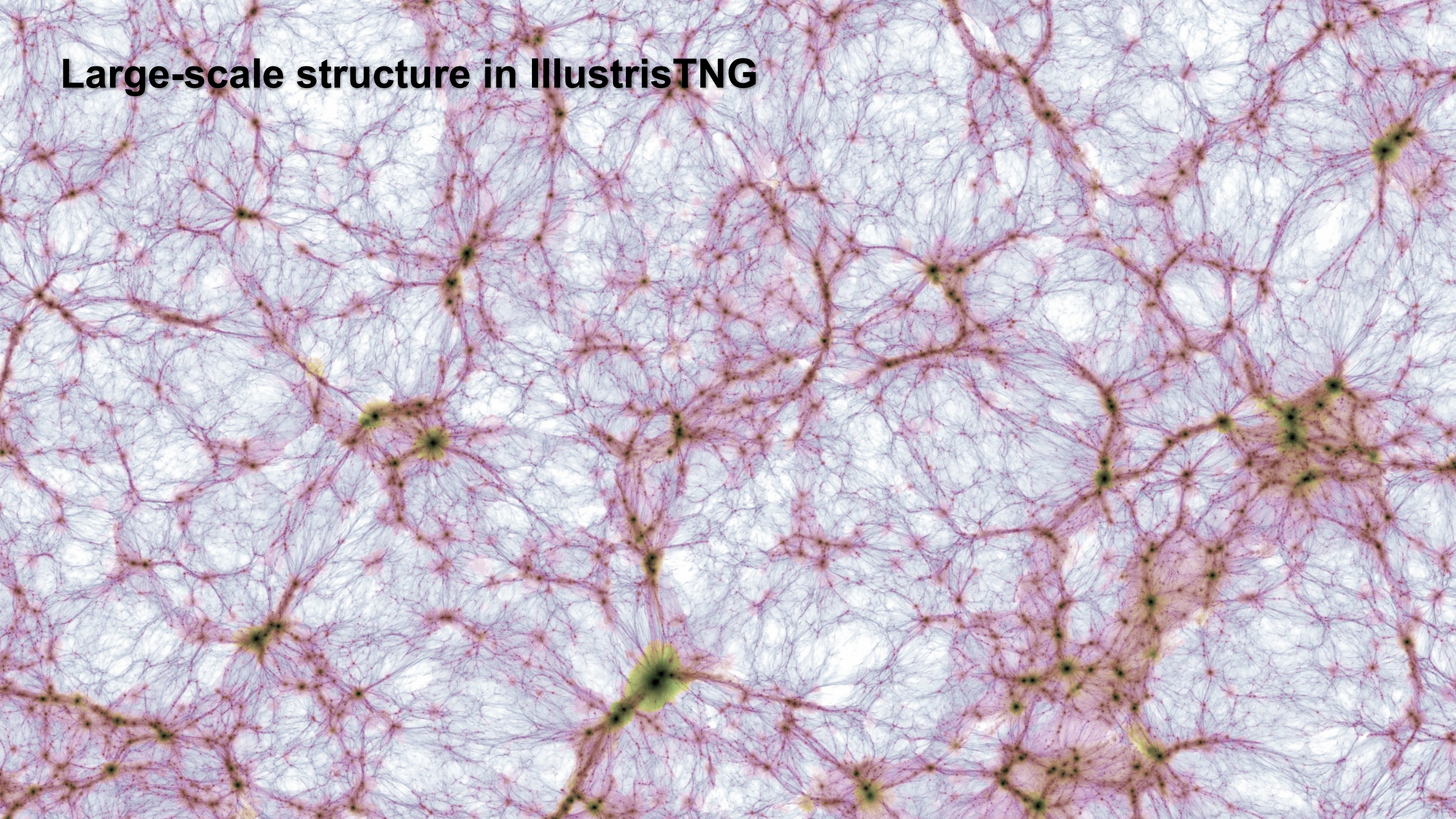

IllustrisTNG predicts galaxy correlation functions in good agreement with the most accurate galaxy surveys

PROJECTED TWO-POINT FUNCTIONS IN DIFFERENT MASS BINS

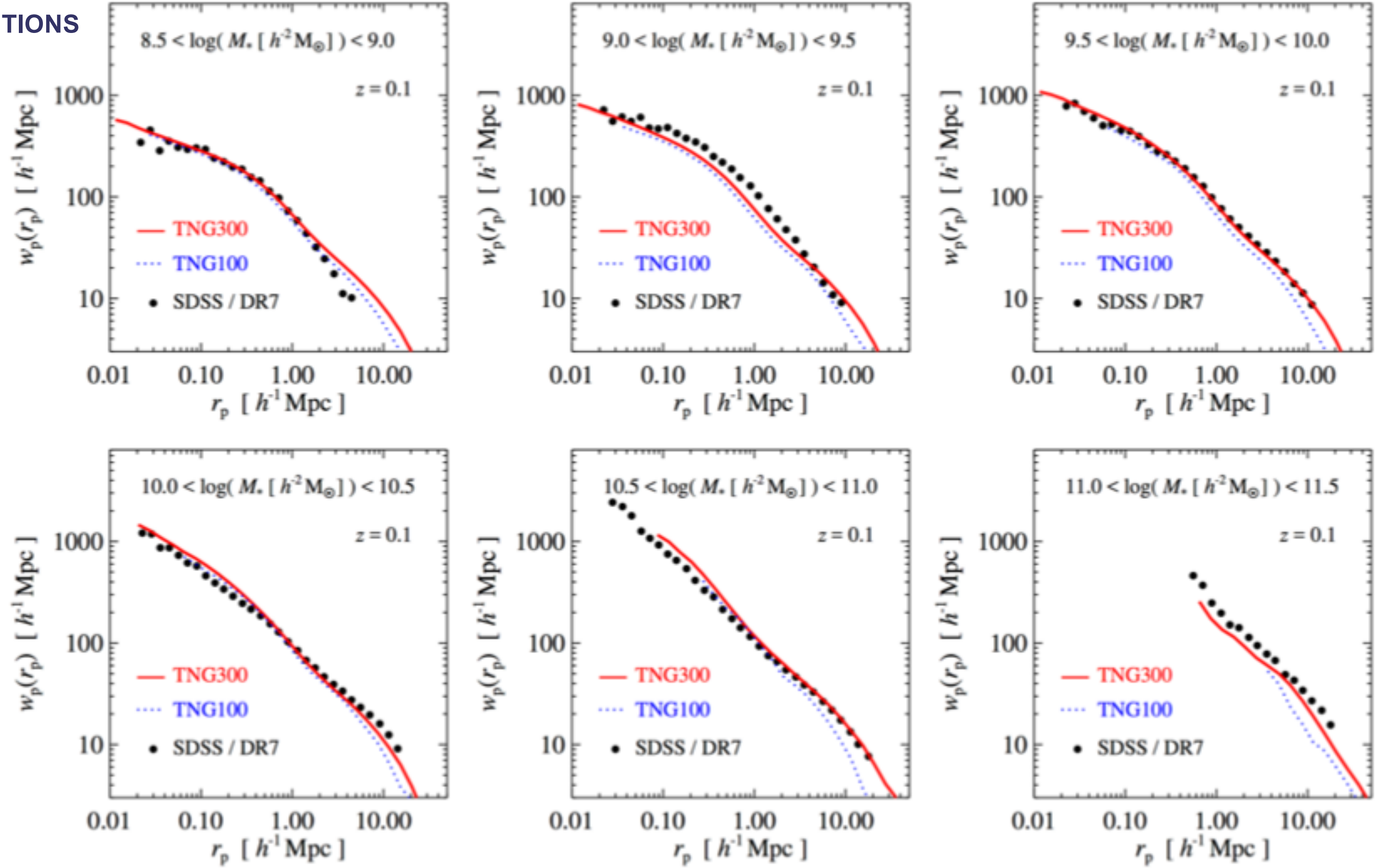

Springel et al. (2018)

IllustrisTNG predicts pronounced differences in the clustering of red and blue galaxies in good agreement with data

CLUSTERING IN DIFFERENT MASS AND COLOR BINS COMPARED TO SDSS

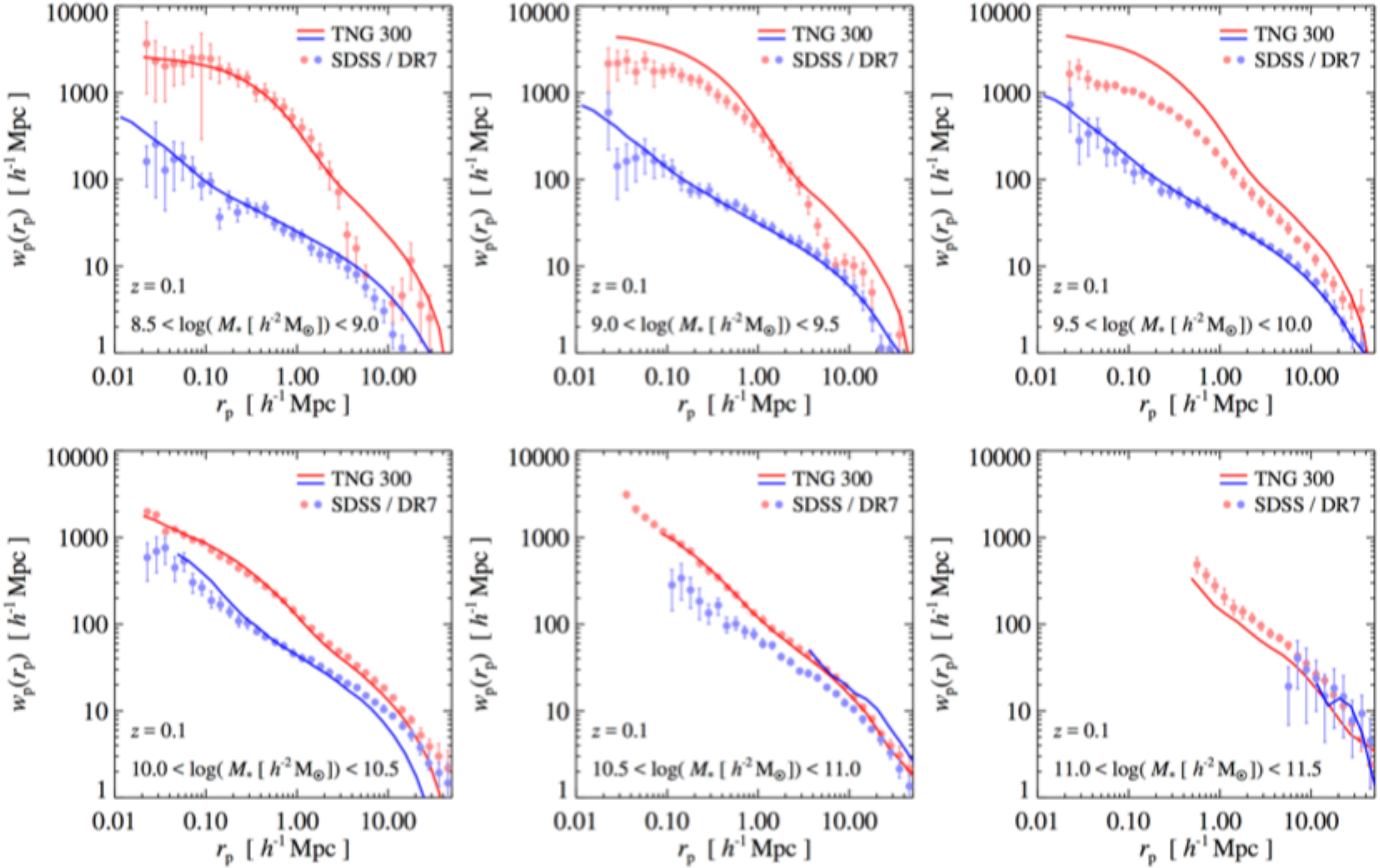

Springel et al. (2018)

The dynamic range challenge

- Only a small range of scales can be addressed in any given simulation
- Only a subset of the relevant physics can be included
- Stellar and AGN feedback couples back to gas-dynamics on larges scales

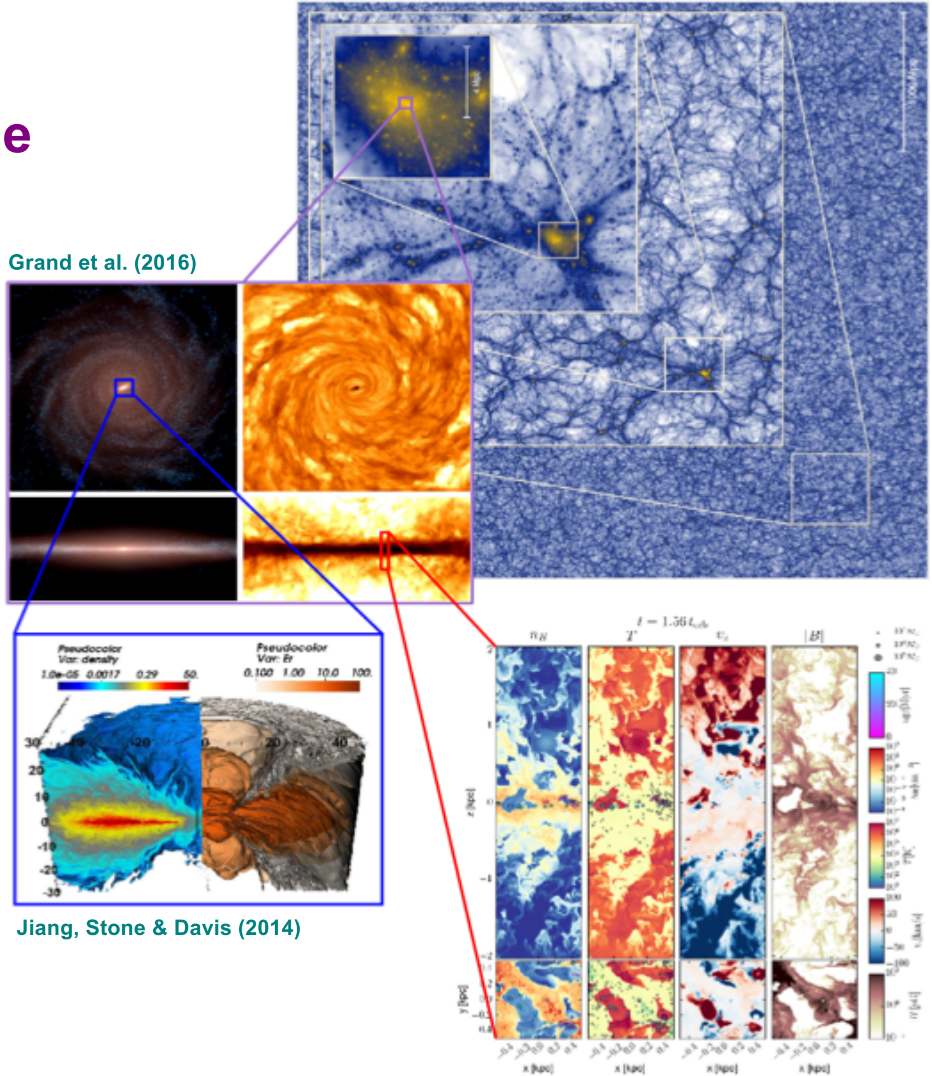

Grand et al. (2016)

Angulo et al. (2012)

Jiang, Stone & Davis (2014)

Kim & Ostriker (2016)

Supermassive Black Holes

Black hole energetics suggests that they could influence the evolution of galaxies

COMPARING SUPERNOVA AND BLACK HOLE ENERGIES

Quasars release plenty of energy

$$L_Q \sim 10^{12}\, L_\odot \qquad t_Q \sim 10^7 - 10^8\,\mathrm{yr}$$

$$E_Q \sim 10^{60} - 10^{61}\,\mathrm{erg}$$

a billion supernovae !

Total available feedback energy from BHs is comparable to that of supernovae

$$\rho_{\rm BH} \simeq 0.001\,\rho_\star \qquad E_{\rm BH}/V \simeq 0.1\,\rho_{\rm BH}\,c^2$$

$$E_{\rm SN}/V \simeq \frac{10^{51}\,\mathrm{erg}}{100\,\mathrm{M}_\odot}\,\rho_\star \qquad \frac{E_{\rm BH}}{E_{\rm SN}} \simeq 1.8$$

But how does AGN energy couple to halo gas?

quasars / AGN

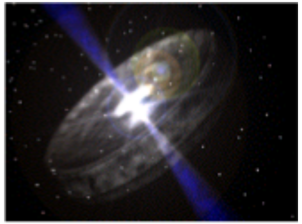

What's the connection?

galaxies

Bondi growth and thermal feedback can self-regulate supermassive black hole growth

A SIMPLE MODEL FOR QUASAR FEEDBACK

Di Matteo, Springel & Hernquist (2005)   Springel, Di Matteo & Hernquist (2005)

Growth of Black Holes

Bondi-Hoyle-Lyttleton type accretion rate parameterization:

$$\dot{M}_{\rm B} = \alpha \times 4\pi R_{\rm B}^2 \, \rho \, c_s \simeq \frac{4\pi\alpha G^2 M_\bullet^2 \, \rho}{(c_s^2 + v^2)^{3/2}}$$

Limitation by the Eddington rate:

$$\dot{M}_\bullet = \min(\dot{M}_{\rm B}, \dot{M}_{\rm Edd})$$

Feedback by Black Holes

Standard radiative efficiency:

$$L_{\rm bol} = 0.1 \times \dot{M}_\bullet \, c^2$$

Coupling of a small fraction of energy output to ambient gas:

$$\dot{E}_{\rm feedback} = f \times L_{\rm bol} \qquad\qquad f \simeq 5\%$$

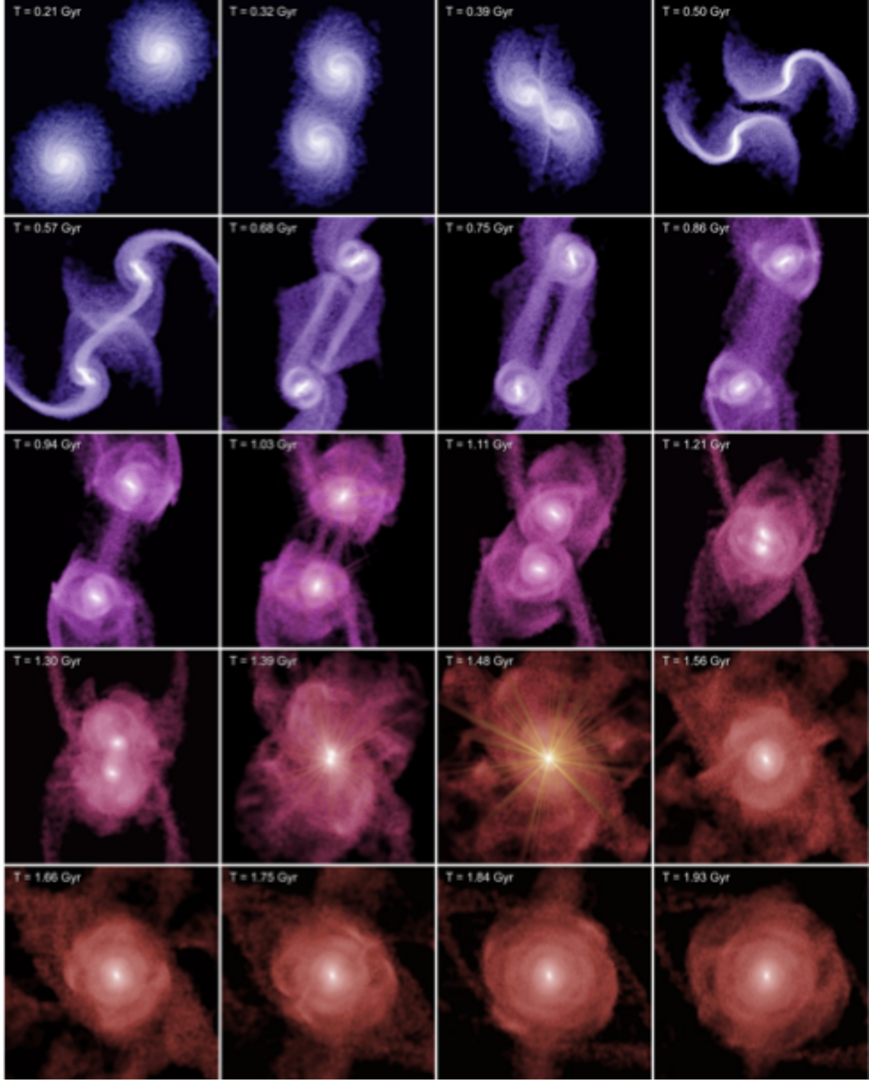

Winds from supermassive black holes may keep ‘red geyser’ galaxies turned off

EXAMPLE OF OBSERVATIONAL EVIDENCE FOR BLACK HOLE WINDS

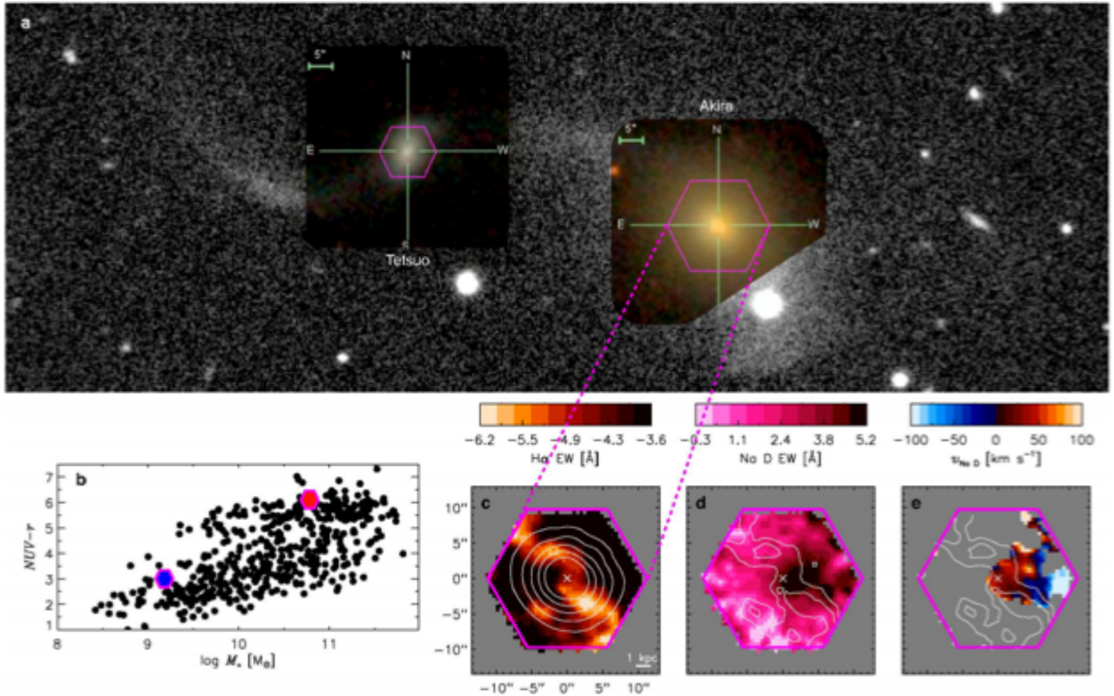

Cheung et al. (2016, Nature, 533, 504)

Genzel et al. (2014), Förster Schreiber et al. (2014)

We used this as motivation for the IllustrisTNG black hole feedback model, and distinguish a “high” and a “low” accretion flow state:

$$\frac{\dot{M}_{\mathrm{Bondi}}}{\dot{M}_{\mathrm{Edd}}} \geq \chi = \min\left[\chi_0 \left(\frac{M_{\mathrm{BH}}}{10^8\,\mathrm{M}_\odot}\right)^{\beta}, 0.1\right]$$

Pure thermal feedback in “high” quasar mode:

$$\Delta\dot{E}_{\mathrm{high}} = \epsilon_{\mathrm{f,high}}\epsilon_{\mathrm{r}}\dot{M}_{\mathrm{BH}}\,c^2$$

Pure kinetic feedback in “low” radio mode:

$$\Delta\dot{E}_{\mathrm{low}} = \epsilon_{\mathrm{f,kin}}\dot{M}_{\mathrm{BH}}c^2.$$

Weinberger et al. (2017)

Massive galaxies are quenched inside–out in HST-3D/CANDELS and IllustrisTNG

COMPARISON OF STACKED SPECIFIC STAR FORMATION MAPS AND THEIR PROFILES AT Z~1

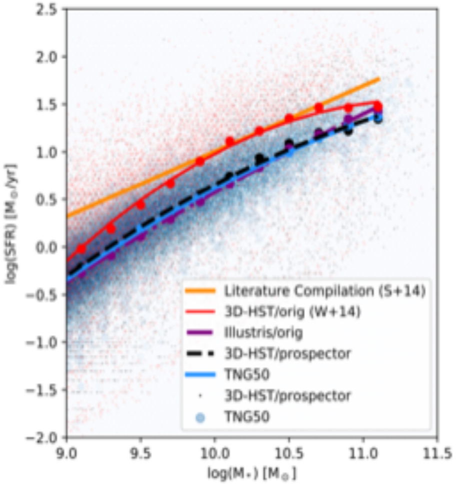

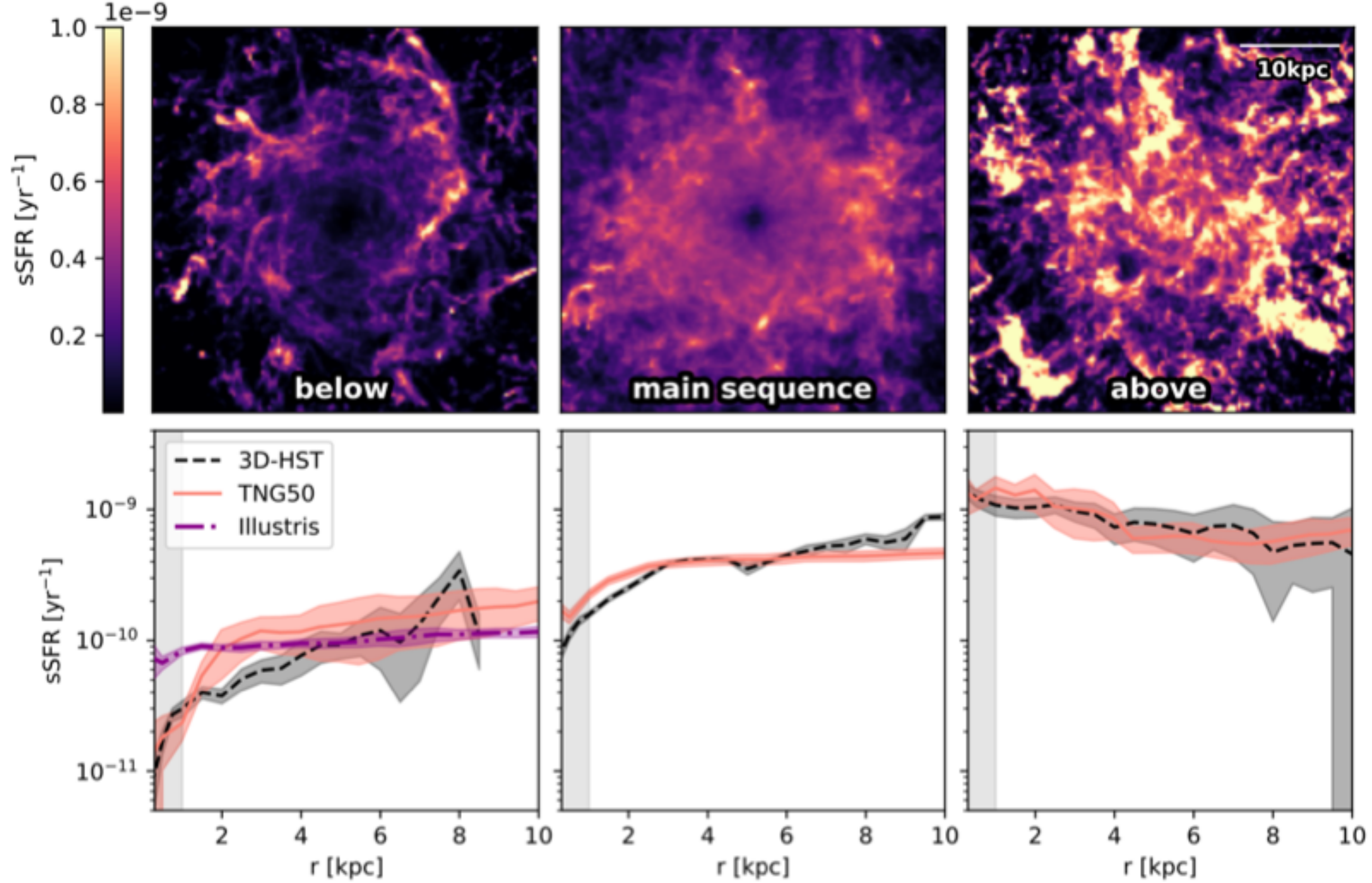

Erica Nelson, et al. (2021)

Strong bimodal outflows arise as an emergent phenomenon from the AGN feedback in TNG

TIME SEQUENCE OF GAS DENSITY AND METALLICITY DISTRIBUTION AROUND AN AGN AT Z~2

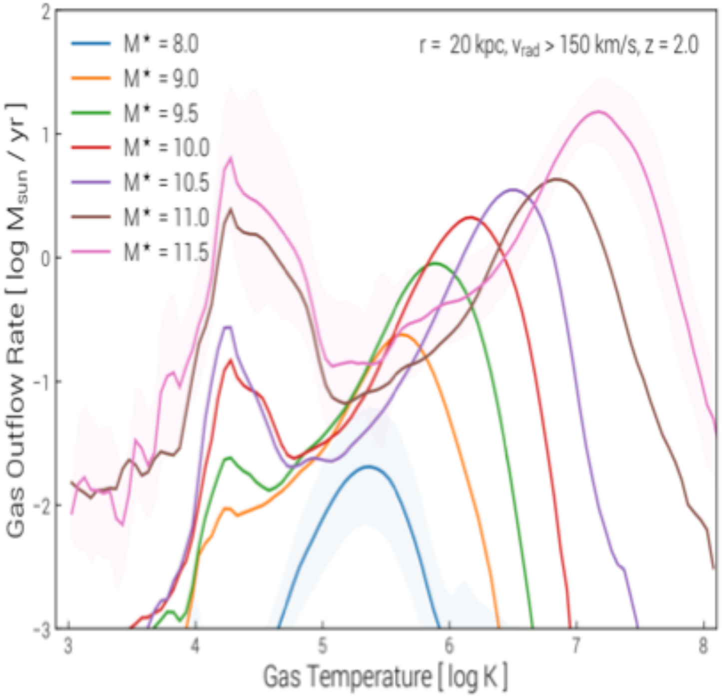

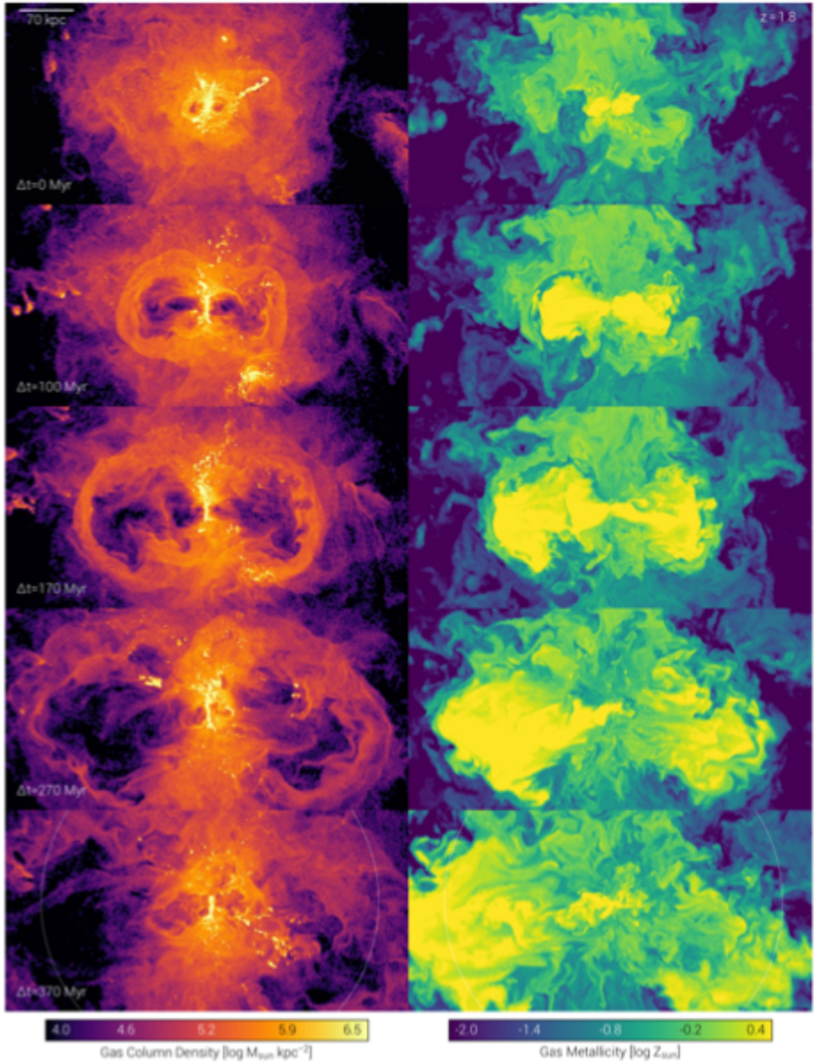

Nelson et al. (2019)

Quenched satellites are more commonly found along the *major axis* and less often along the *minor axis* around central galaxies in SDSS

DIRECTIONALLY QUENCHED SDSS SATELLITES

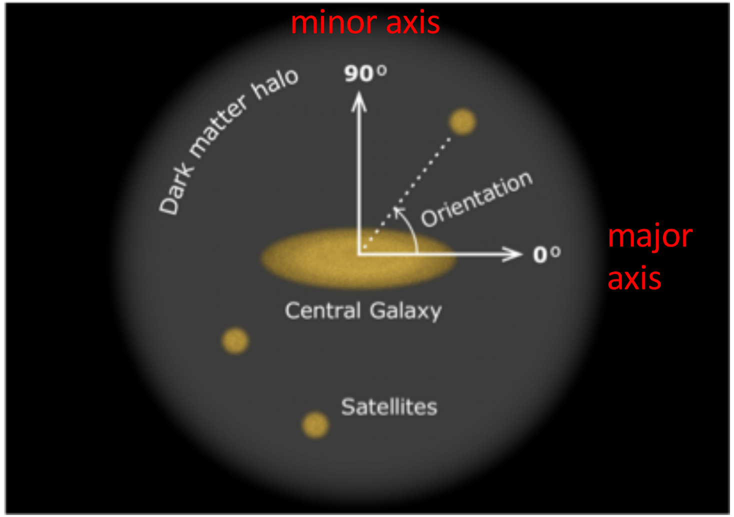

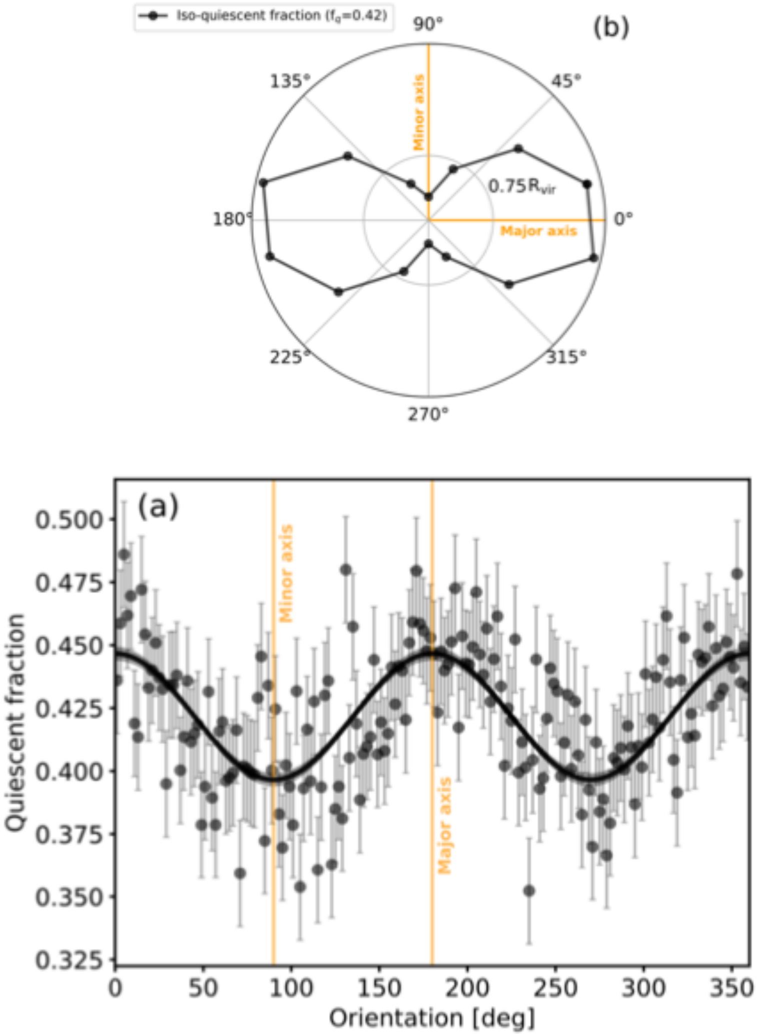

Ignacio Martin-Navarro, et al. (2021)

The directional quenching is accurately reproduced by TNG – as an indirect effect of its AGN feedback

QUIESCENT SATELLITES IN SDSS AND TNG, AND CGM DENSITY MODULATION IN TNG

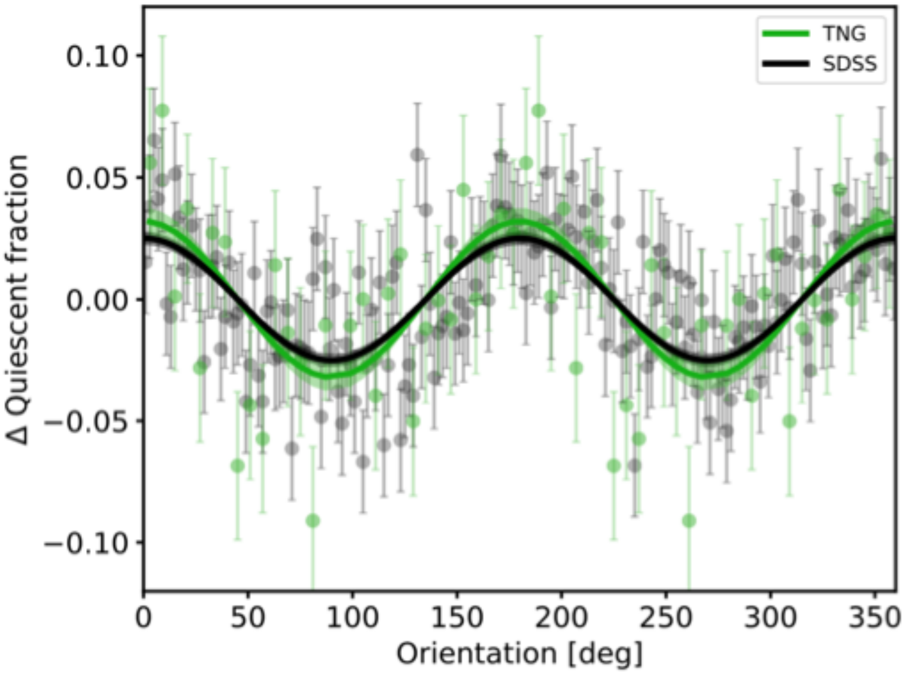

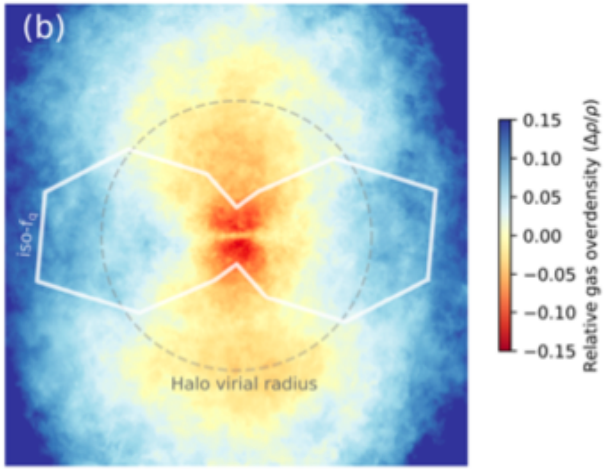

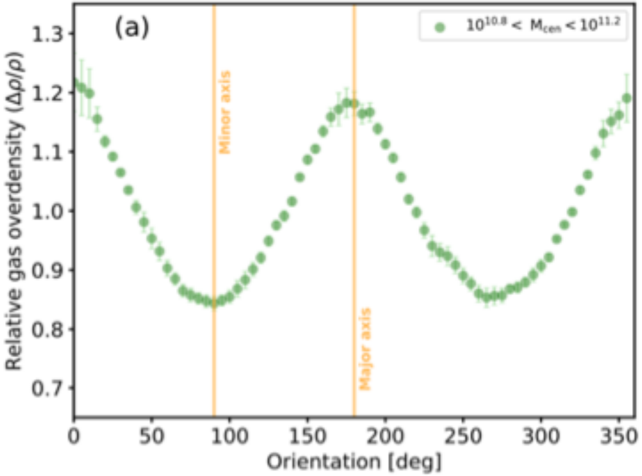

Ignacio Martin-Navarro, et al. (2021)

Even X-ray / γ-ray bubbles in disk galaxies readily arise from simple *isotropic* AGN feedback models

SLICES THROUGH DISK GALAXY SIMULATIONS

Costa, Pakmor & Springel (2021)

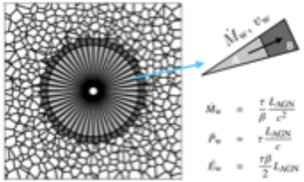

$$\dot{M}_w = \frac{\tau}{\beta}\frac{L_{\rm AGN}}{c^2}$$
$$\dot{P}_w = \tau\frac{L_{\rm AGN}}{c}$$
$$\dot{E}_w = \frac{\tau\beta}{2}L_{\rm AGN}$$

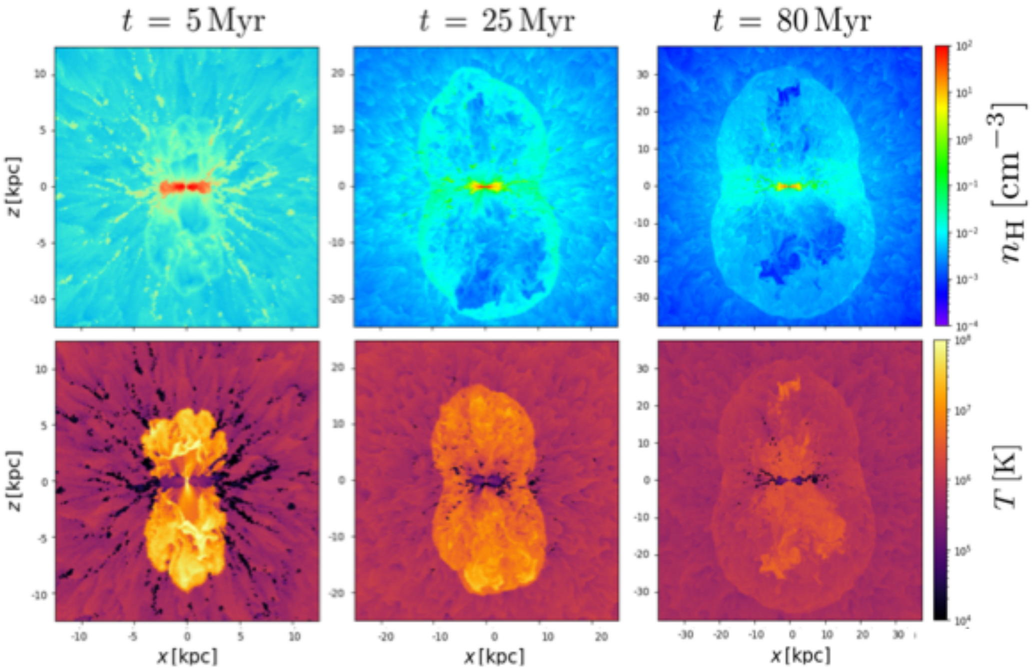

Pillepich et al. (2021)

AGN bubbles in TNG50

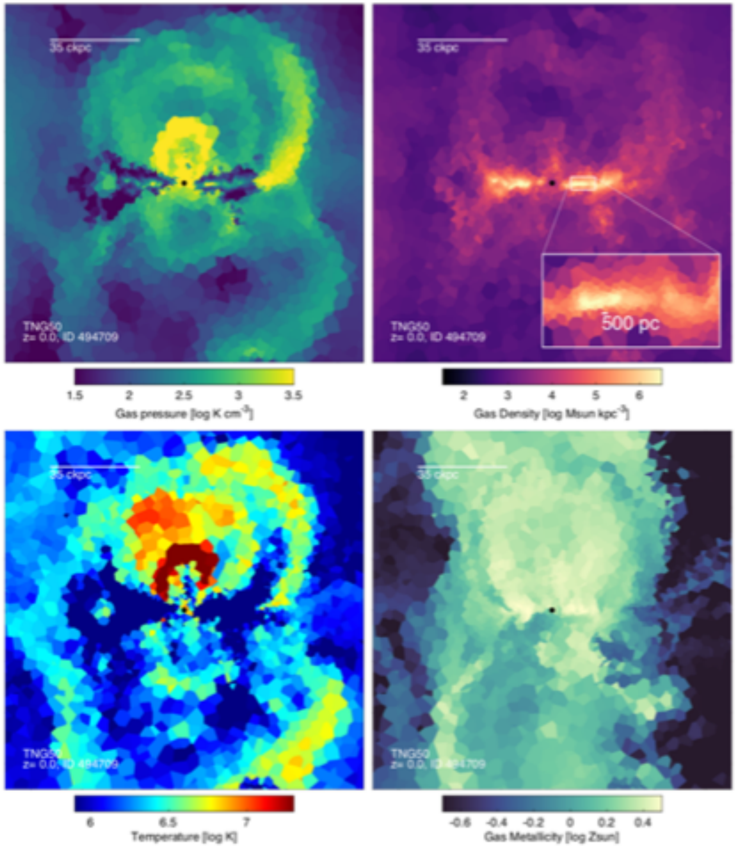

Magnetic field predictions

Modern MHD simulations of galaxy formation can predict the amplification of primordial fields in halos and galaxies

MAGNETIC FIELD STRENGTH IN AURIGA AND ILLUSTRIS-TNG

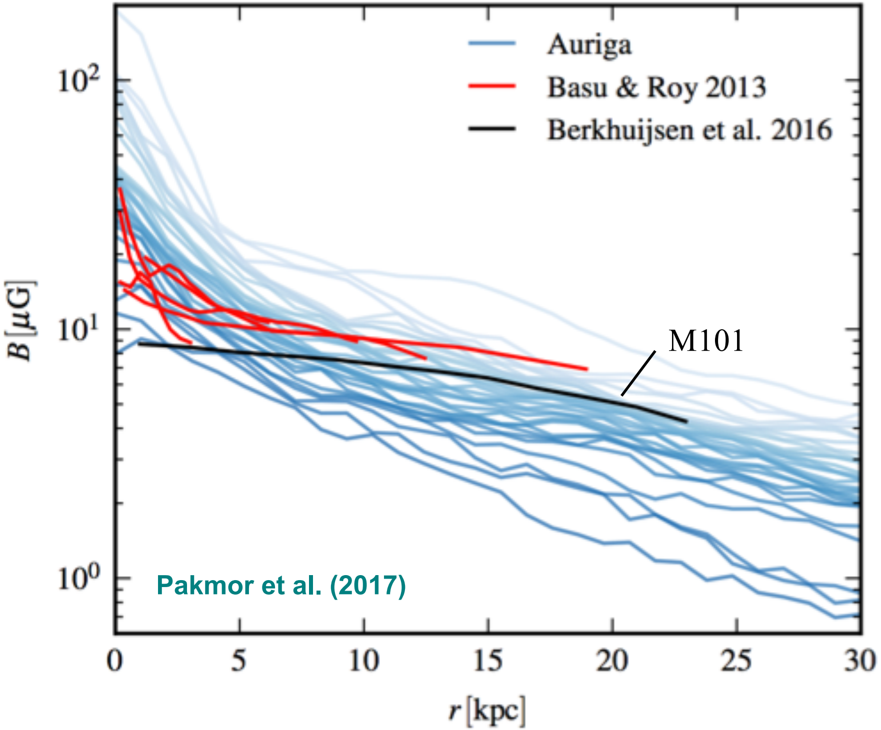

Pakmor et al. (2017)

Marinacci et al. (2018)

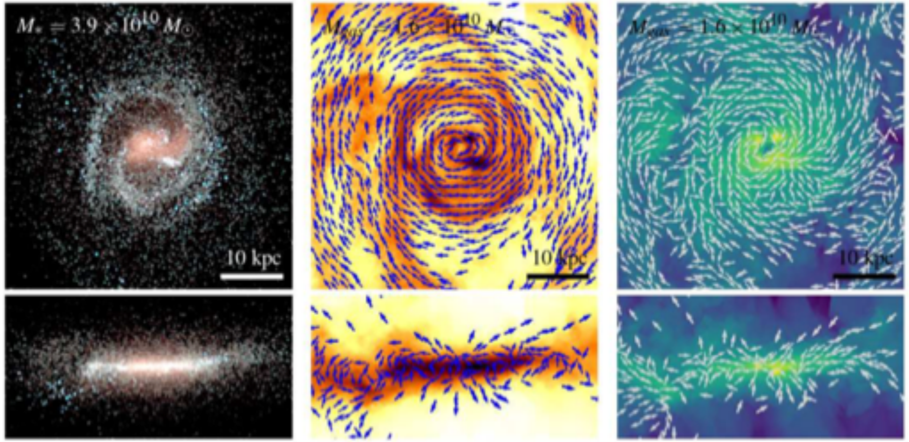

Amplification of B-field occurs through turbulent small-scale dynamo

Pakmor et al. (2017, 2019)

EVOLUTION OF VELOCITY AND B-FIELD POWER SPECTRA

Small-scale subsonic turbulent dynamo in action:

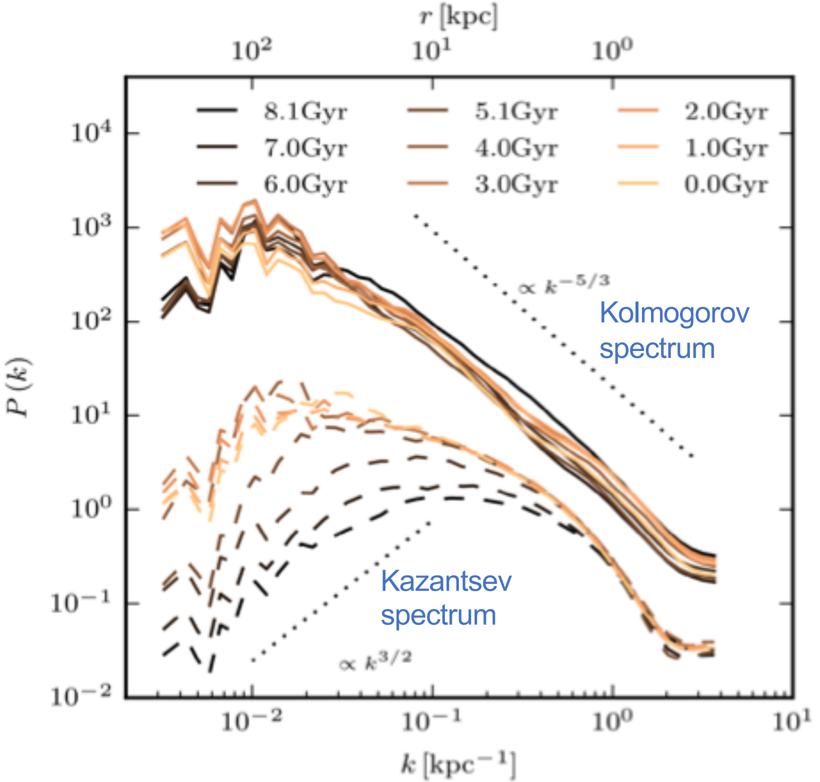

Kolmogorov spectrum

Kazantsev spectrum

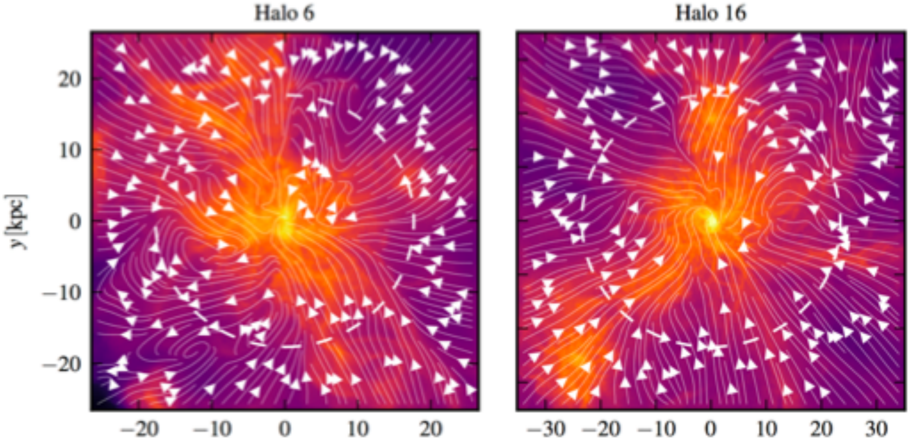

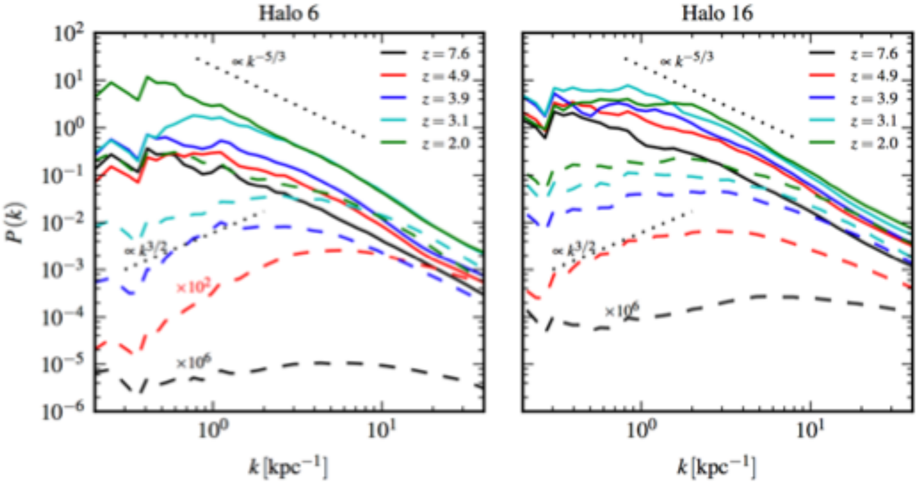

Faraday rotation maps provide one of the best ways to observationally probe the magnetic field in galaxies

COSMOLOGICAL PREDICTIONS FROM AURIGA COMPARED TO OBSERVATIONS OF M51

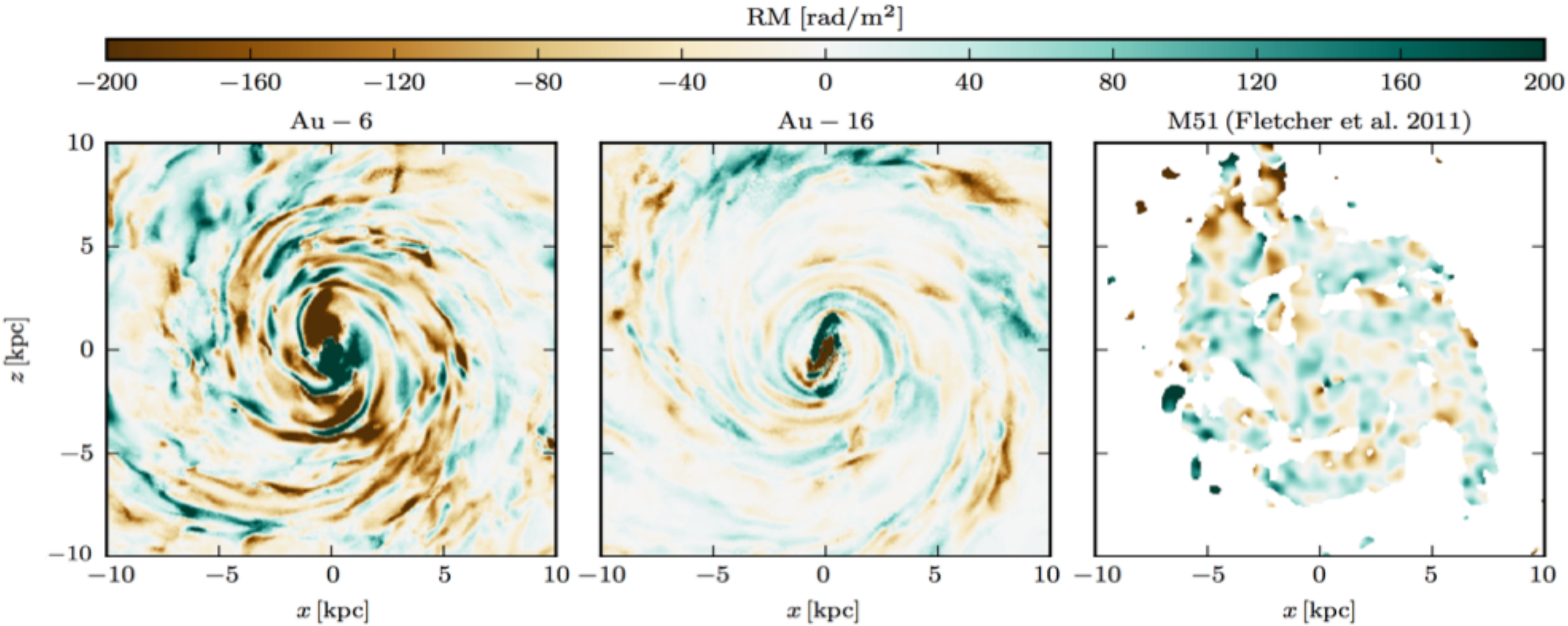

$$RM = \frac{e^3}{2\pi m_e^2 c^3} \int n_e(l)\, \vec{B}(l) \cdot d\vec{l},$$

Pakmor et al. (2018)

Cosmic rays

How can galaxies shed a substantial fraction of their baryonic content?

FLOWS IN THE CIRCUM-GALACTIC MEDIUM IN A GALAXY FROM THE TNG-50 SIMULATION

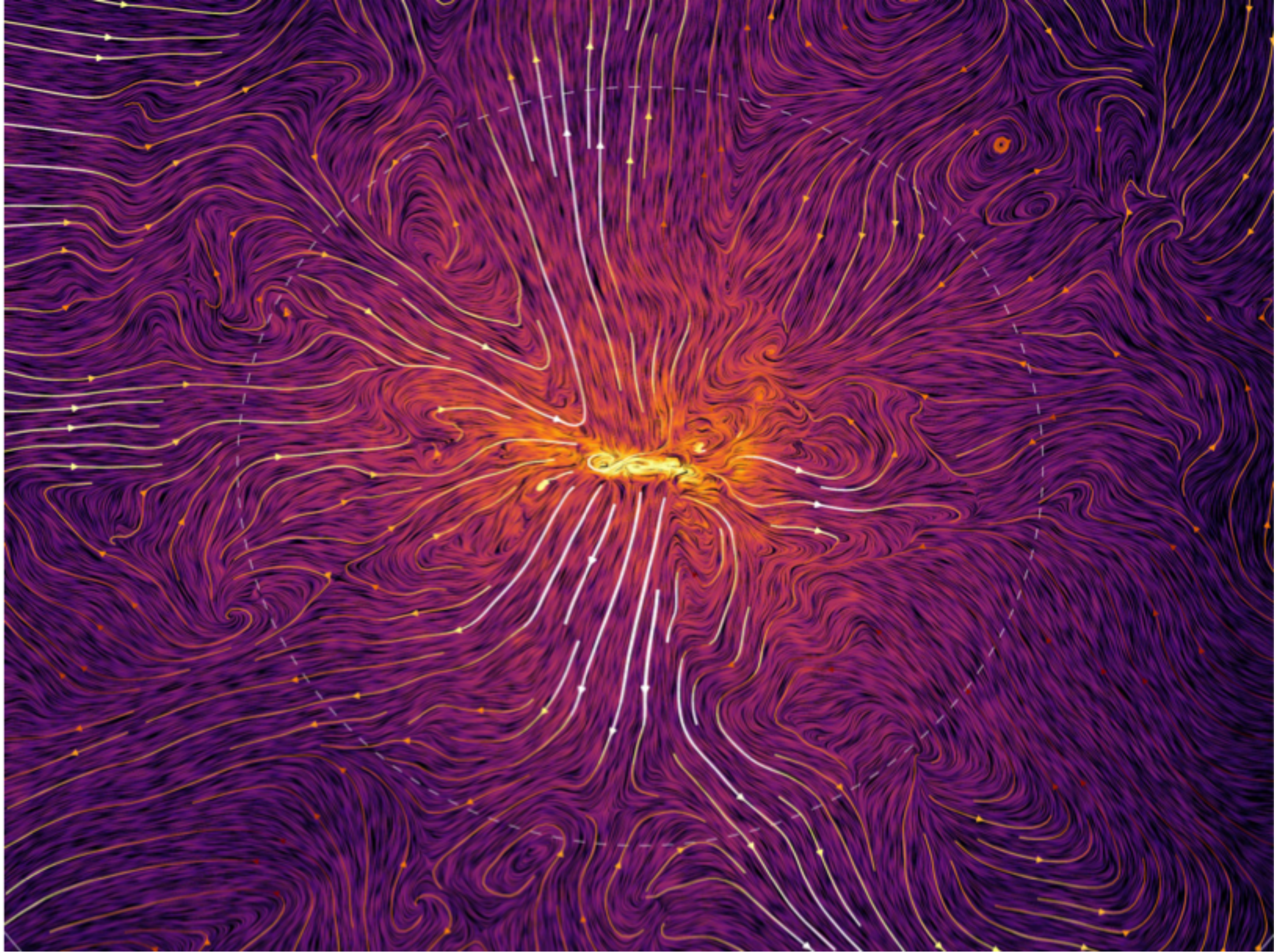

Nelson et al. (2019)

The Galactic cosmic ray energy spectrum provides a significant contribution to the total ISM pressure

GLOBAL PROPERTIES OF GALACTIC COSMIC RAYS

Approximation as an isotropic power-law in momentum

$$f(p) = \frac{\mathrm{d}N}{\mathrm{d}p\,\mathrm{d}V} = C\,p^{-\alpha}\theta(p-q)$$

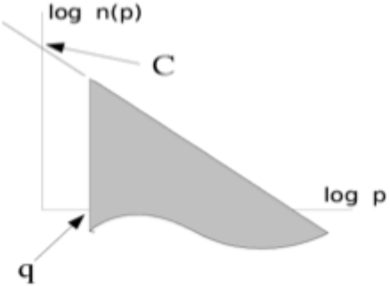

$$P_{\mathrm{CR}} = \frac{C\,m_{\mathrm{p}}c^2_{\mathrm{light}}}{6}\,\mathcal{B}_{\frac{1}{1+q^2}}\left(\frac{\alpha-2}{2}, \frac{3-\alpha}{2}\right)$$

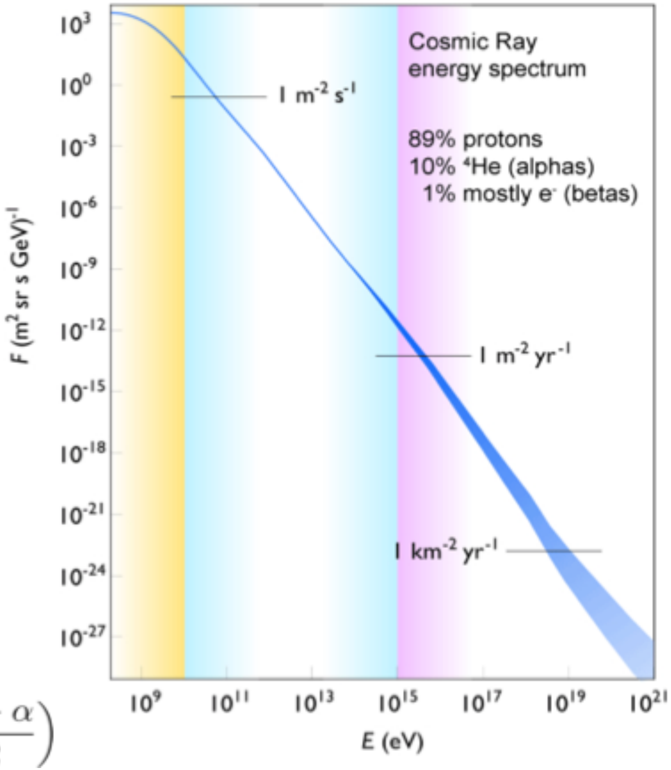

data compiled by Swordy

energy density in cosmic rays:
comparable to thermal and magnetic energy densities in ISM (equipartition)

main production mechanisms:

- supernova shocks (10-30% of the energy appears as CRs)
- large-scale structure formation shocks

main dissipation mechanisms:

- Coulomb losses
- hadronic interactions, mostly pion production
- Bremsstrahlung (negligible for protons)

Cosmic rays can drive galactic winds when coupled with transport processes

DISK SIMULATIONS BY DIFFERENT GROUPS

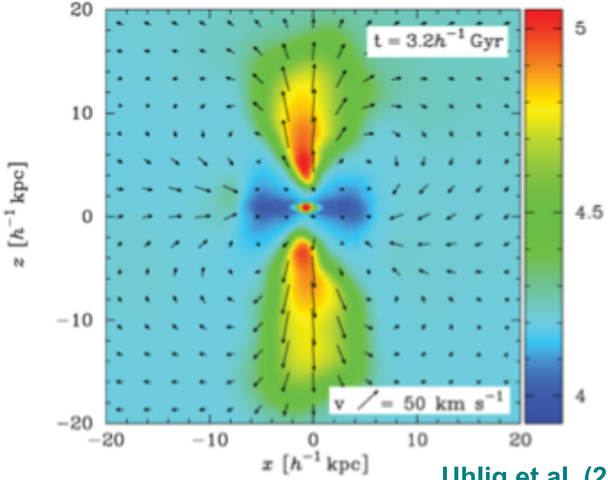

Uhlig et al. (2012)

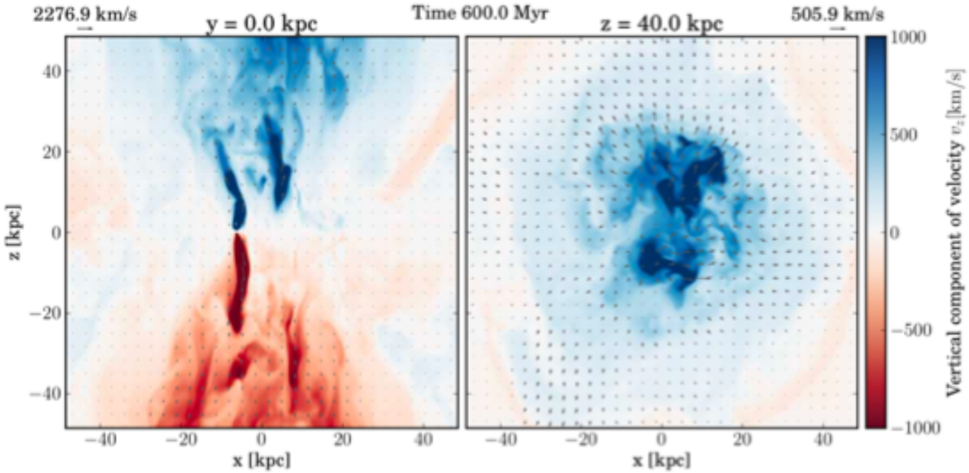

Hanasz et al. (2013)

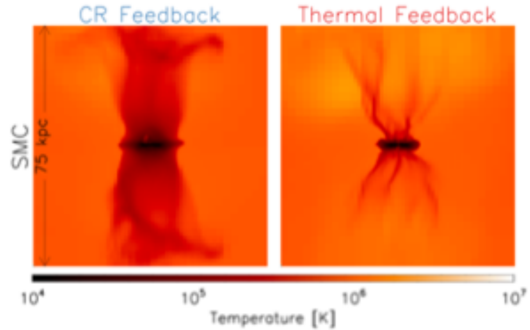

Booth et al. (2013)

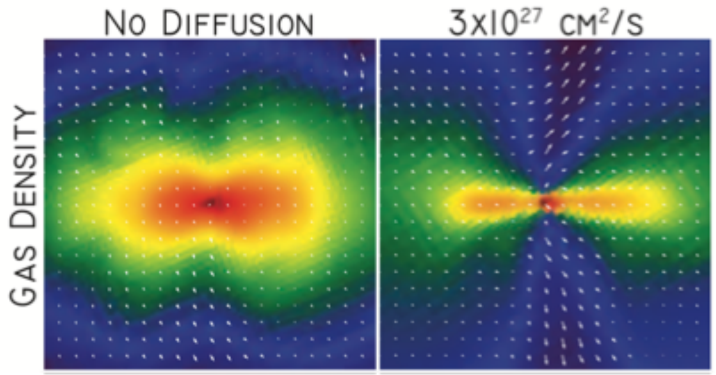

Salem et al. (2014)

Adding cosmic rays to galaxy formation simulations makes the dynamic range problem much harder

GYRO-RADIUS COMPARED TO THE SIZE OF A GALAXY

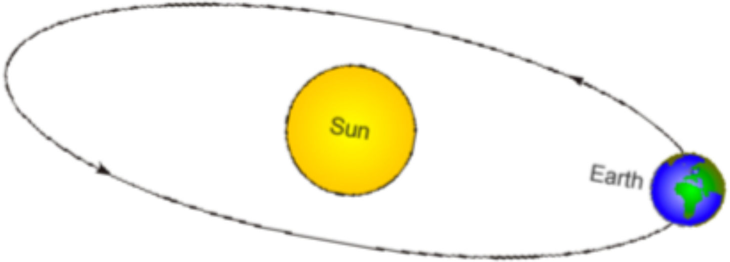

Milky Way-like galaxy:

$$r_{\mathrm{gal}} \sim 10^4 \text{ pc}$$

gyro-orbit of GeV cosmic ray:

$$r_{\mathrm{cr}} = \frac{p_\perp}{e\,B_{\mu\mathrm{G}}} \sim 10^{-6} \text{ pc} \sim \frac{1}{4} \text{ AU}$$

→ **Need to develop an effective two-fluid theory that can be treated with hydrodynamical methods**

Transport of CRs relative to the thermal energy is required to set-up wind-driving CR gradients in the low density halo

MECHANISM OF COSMIC-RAY DRIVEN WINDS

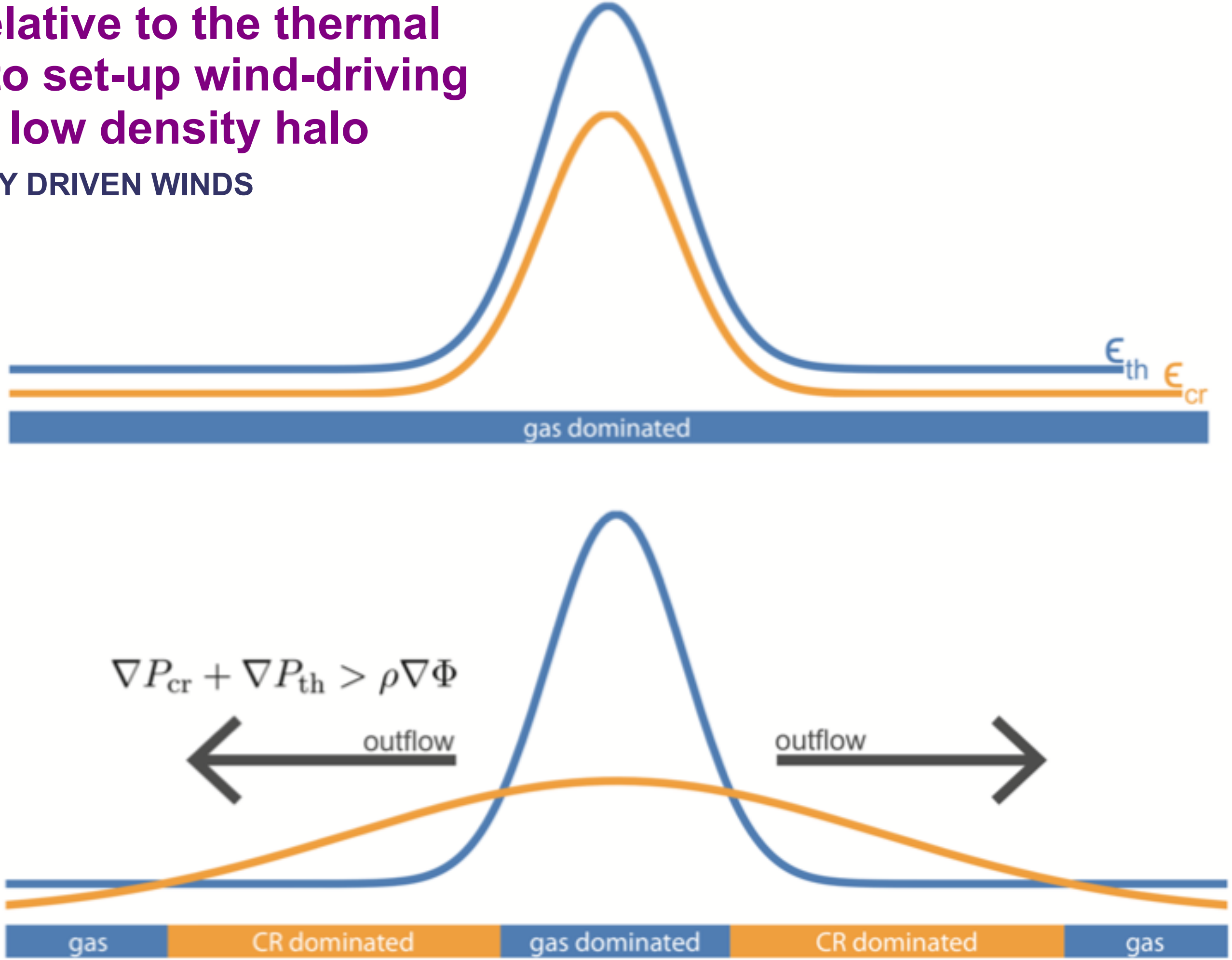

Salem & Bryan (2014)

CR dynamics and transport complicates fluid dynamics considerably

COSMIC RAY DYNAMICS WITHOUT SOURCE AND SINK TERMS

$$\frac{\partial \boldsymbol{U}}{\partial t} + \boldsymbol{\nabla}\cdot \mathsf{F} = \boldsymbol{S}$$

$$\boldsymbol{U} = \begin{pmatrix} \rho \\ \rho\boldsymbol{v} \\ \varepsilon \\ \varepsilon_{\mathrm{cr}} \\ \boldsymbol{B} \end{pmatrix}, \quad \mathsf{F} = \begin{pmatrix} \rho\boldsymbol{v} \\ \rho\boldsymbol{v}\boldsymbol{v}^{\mathrm{T}} + P\mathbf{1} - \boldsymbol{B}\boldsymbol{B}^{\mathrm{T}} \\ (\varepsilon + P)\boldsymbol{v} - \boldsymbol{B}\,(\boldsymbol{v}\cdot\boldsymbol{B}) \\ \varepsilon_{\mathrm{cr}}\boldsymbol{v} + (\varepsilon_{\mathrm{cr}} + P_{\mathrm{cr}})\boldsymbol{v}_{\mathrm{st}} - \kappa_{\varepsilon}\boldsymbol{b}\,(\boldsymbol{b}\cdot\boldsymbol{\nabla}\varepsilon_{\mathrm{cr}}) \\ \boldsymbol{B}\boldsymbol{v}^{\mathrm{T}} - \boldsymbol{v}\boldsymbol{B}^{\mathrm{T}} \end{pmatrix}, \quad \boldsymbol{S} = \begin{pmatrix} 0 \\ \mathbf{0} \\ P_{\mathrm{cr}}\,\boldsymbol{\nabla}\cdot\boldsymbol{v} - \boldsymbol{v}_{\mathrm{st}}\cdot\boldsymbol{\nabla}P_{\mathrm{cr}} + \Lambda_{\mathrm{th}} + \Gamma_{\mathrm{th}} \\ -P_{\mathrm{cr}}\,\boldsymbol{\nabla}\cdot\boldsymbol{v} + \boldsymbol{v}_{\mathrm{st}}\cdot\boldsymbol{\nabla}P_{\mathrm{cr}} + \Lambda_{\mathrm{cr}} + \Gamma_{\mathrm{cr}} \\ \mathbf{0} \end{pmatrix}$$

$$P = P_{\mathrm{th}} + P_{\mathrm{cr}} + \frac{\boldsymbol{B}^2}{2} \qquad \varepsilon = \varepsilon_{\mathrm{th}} + \frac{\rho\boldsymbol{v}^2}{2} + \frac{\boldsymbol{B}^2}{2} \qquad \boldsymbol{v}_{\mathrm{st}} = -\frac{\boldsymbol{B}}{\sqrt{\rho}}\,\mathrm{sgn}(\boldsymbol{B}\cdot\boldsymbol{\nabla}P_{\mathrm{cr}})$$

cosmic ray streaming, nasty(!) numerically

Energy equation:

$$\frac{\partial \varepsilon_{\mathrm{cr}}}{\partial t} + \boldsymbol{\nabla}\cdot\left[\varepsilon_{\mathrm{cr}}(\boldsymbol{v} + \boldsymbol{v}_{\mathrm{st}}) - \kappa_{\varepsilon}\boldsymbol{b}\,(\boldsymbol{b}\cdot\boldsymbol{\nabla}\varepsilon_{\mathrm{cr}})\right] = -P_{\mathrm{cr}}\,\boldsymbol{\nabla}\cdot(\boldsymbol{v} + \boldsymbol{v}_{\mathrm{st}}) + \Lambda_{\mathrm{cr}} + \Gamma_{\mathrm{cr}}$$

anisotropic diffusion

Stratified-box simulations of SN feedback demonstrate the importance of CRs for driving outlows

DIFFERENT MODES OF SUPERNOVA FEEDBACK

with gas self-gravity and
stationary stellar potential

self-shielding with TreeCol

$$\Sigma_0 = 10\ \mathrm{M}_\odot\ \mathrm{pc}^{-2}$$
$$f_g = 0.1$$
$$m_t = 10\ \mathrm{M}_\odot$$
$$\varepsilon = 0.165\ \mathrm{pc}$$

Simpson et al. (2016)

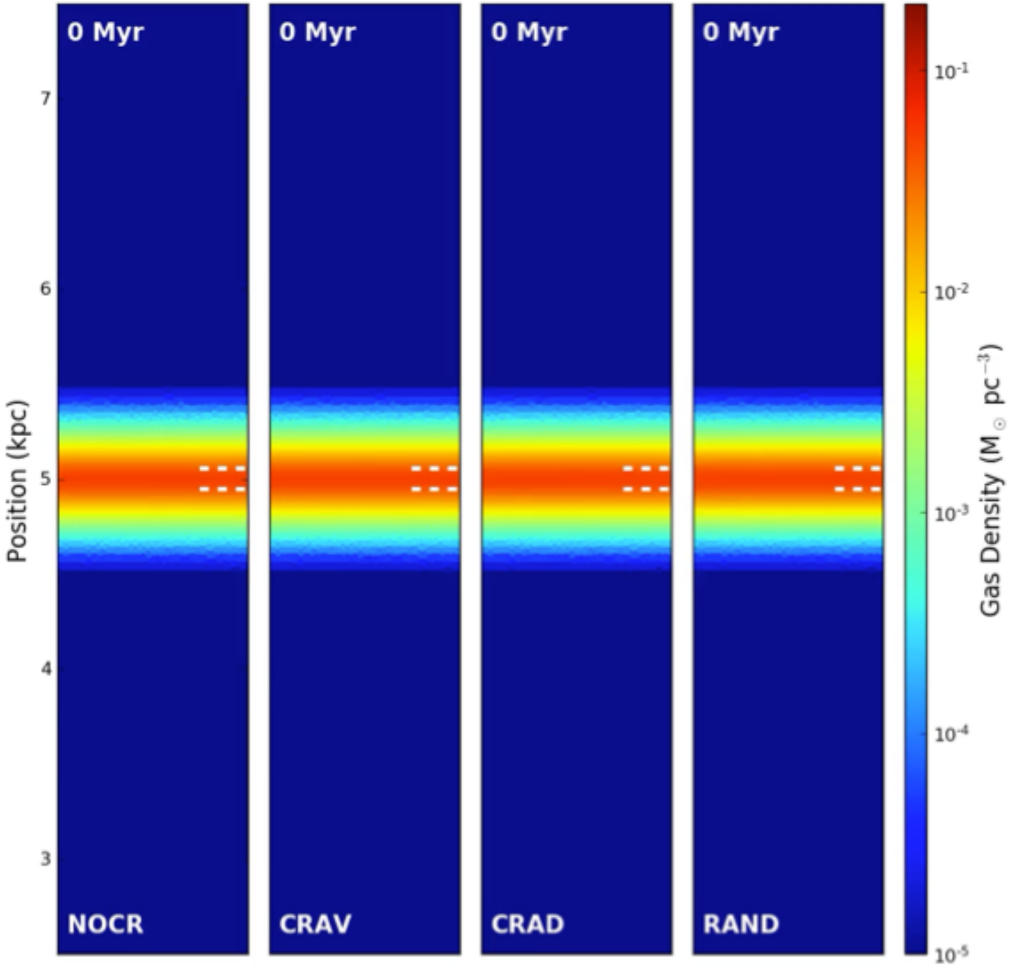

The efficiency of cosmic ray driven winds is a strong function of halo mass

OUTFLOW VELOCITIES IN ISOLATED GALAXIES OF DIFFERENT SIZE

Jacob et al. (2017)

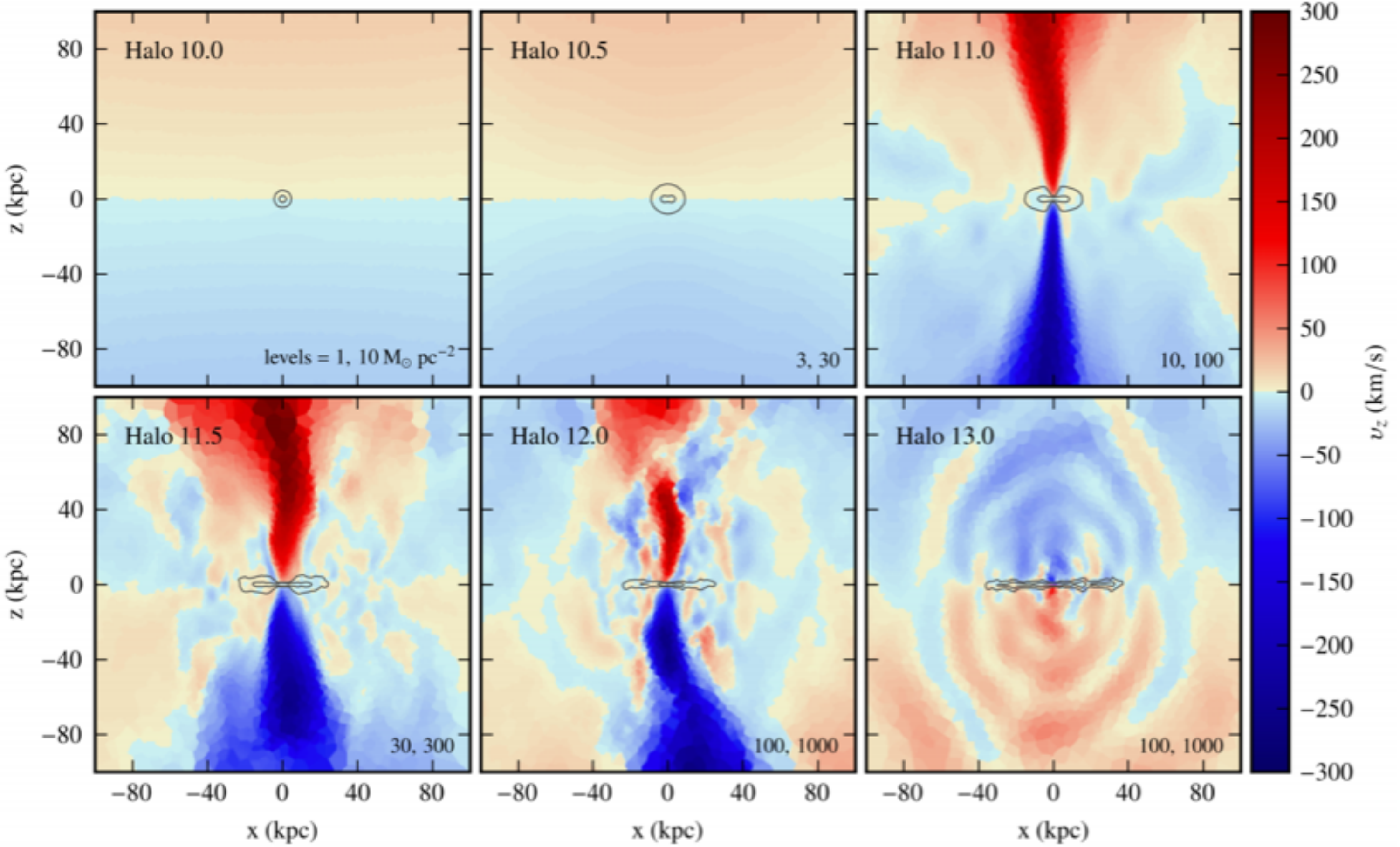

The mass loading of CR-driven winds depends strongly on halo mass, whereas the energy loading is flat

PROPERTIES OF CR DRIVEN WINDS AS A FUNCTION OF HALO MASS

Jacob et al. (2017)

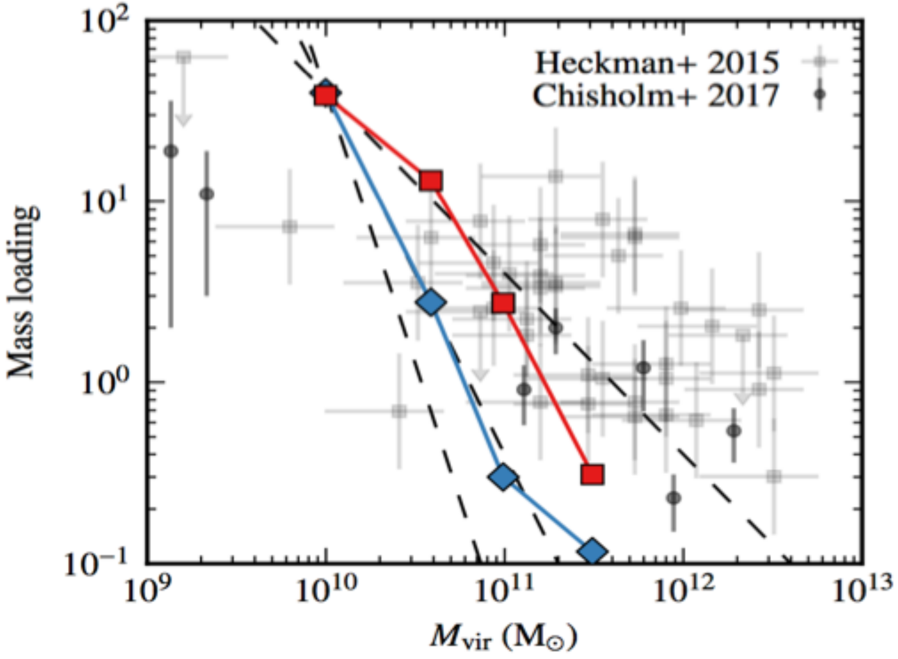

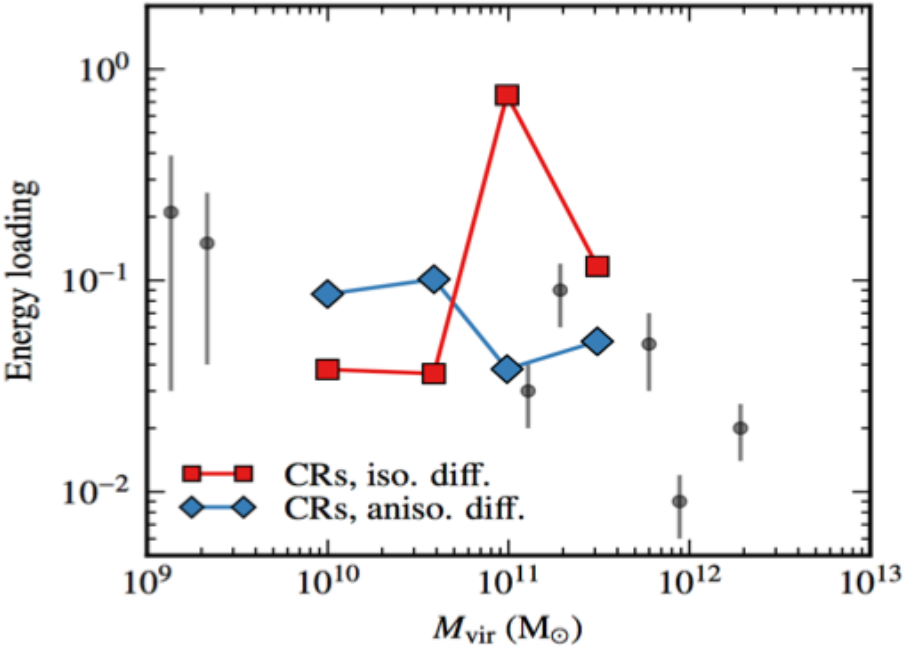

CR-transport changes the disk sizes in cosmological simulations

AURIGA SIMULATIONS WITH DIFFERENT CR PHYSICS

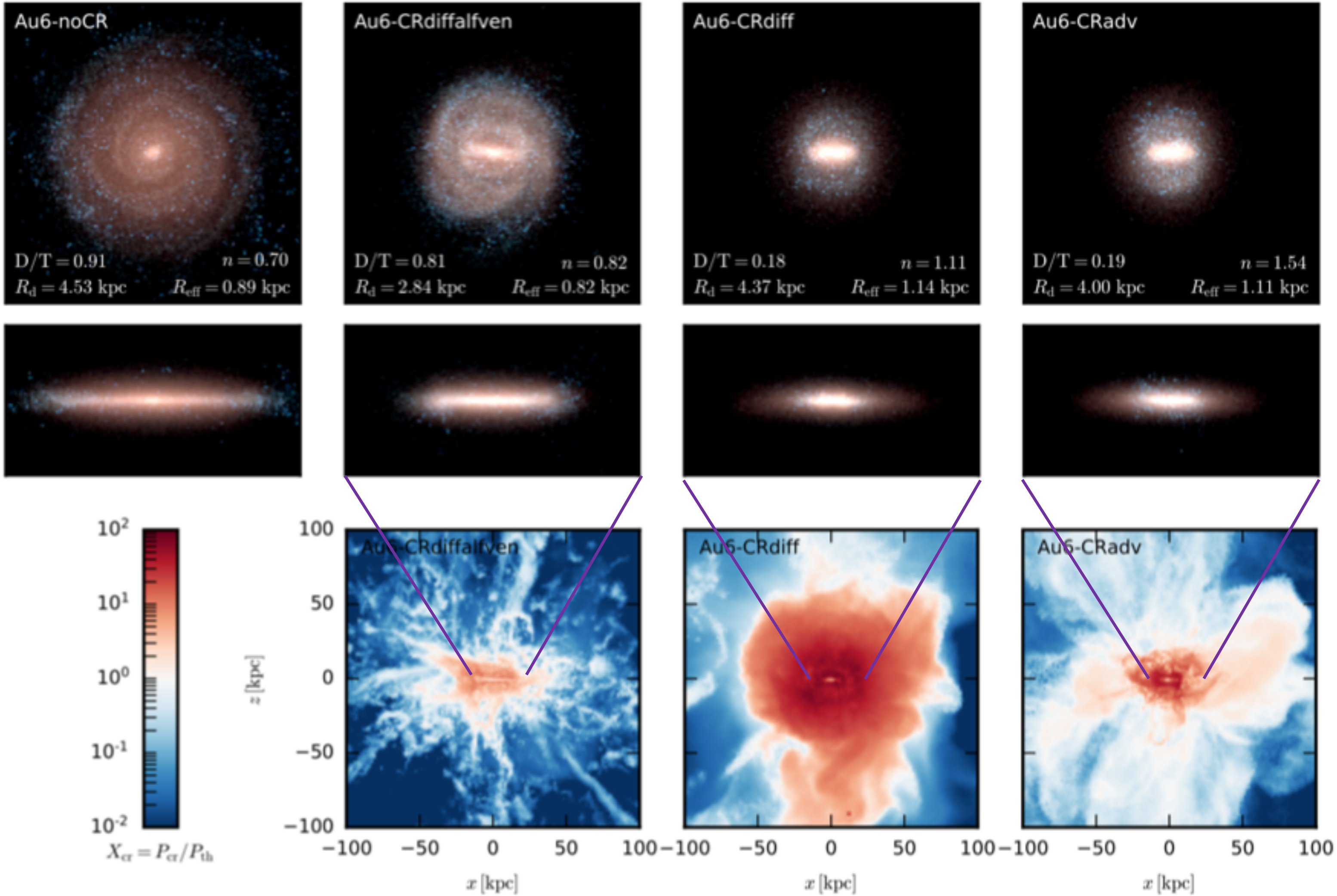

Buck et al. (2019)

Cosmic rays are able to significantly change the flow pattern in the CGM

VELOCITY FIELD IN AURIGA-6 FOR DIFFERENT CR TRANSPORT MODELS

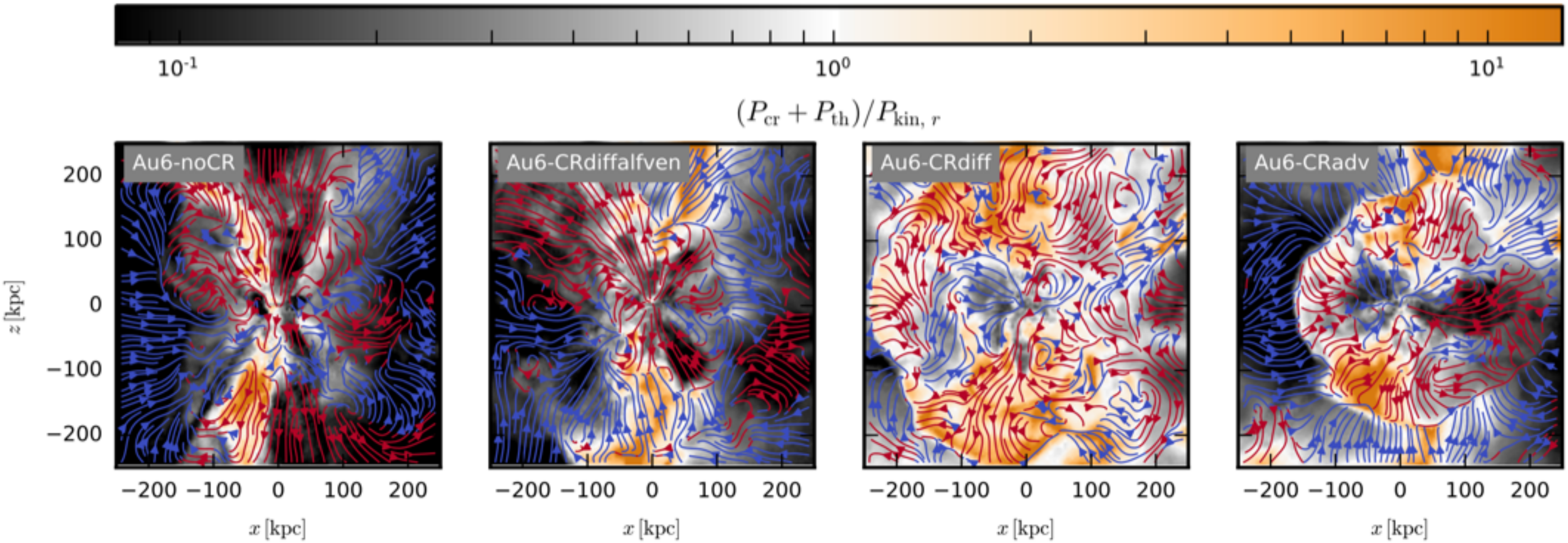

Buck et al. (2019)

- Recent hydrodynamical cosmological simulations have made substantial **progress towards successfully forming galaxies within ΛCDM**.
- These simulations support a picture where **AGN feedback** quenches massive galaxies inside-out.
- The present-day **magnetic fields** in galaxies can arise from a **small-scale dynamo** already at high redshift. The fields are insensitive to the details of magnetogenesis.
- **Cosmic rays** could play an important role in driving galactic outflows in **low-mass galaxies**.
- Future **multi-scale, multi-physics** simulations will be **necessary** to better understand the associated fundamental astrophysical questions.